Annu. Rev. Biophys. Biomol. Struct. 2002. 31:443–84
DOI: 10.1146/annurev.biophys.31.082901.134348

RHODOPSIN: Insights from Recent Structural Studies

Thomas P. Sakmar, Santosh T. Menon, Ethan P. Marin, and Elias S. Awad

Howard Hughes Medical Institute, Laboratory of Molecular Biology and Biochemistry, The Rockefeller University, New York, New York, 10021; e-mail: sakmar@mail.rockefeller.edu

Key Words G protein–coupled receptor, vision, chromophore, retinal, signal transduction

■ **Abstract** The recent report of the crystal structure of rhodopsin provides insights concerning structure-activity relationships in visual pigments and related G protein–coupled receptors (GPCRs). The seven transmembrane helices of rhodopsin are interrupted or kinked at multiple sites. An extensive network of interhelical interactions stabilizes the ground state of the receptor. The ligand-binding pocket of rhodopsin is remarkably compact, and several chromophore-protein interactions were not predicted from mutagenesis or spectroscopic studies. The helix movement model of receptor activation, which likely applies to all GPCRs of the rhodopsin family, is supported by several structural elements that suggest how light-induced conformational changes in the ligand-binding pocket are transmitted to the cytoplasmic surface. The cytoplasmic domain of the receptor includes a helical domain extending from the seventh transmembrane segment parallel to the bilayer surface. The cytoplasmic surface appears to be approximately large enough to bind to the transducin heterotrimer in a one-to-one complex. The structural basis for several unique biophysical properties of rhodopsin, including its extremely low dark noise level and high quantum efficiency, can now be addressed using a combination of structural biology and various spectroscopic methods. Future high-resolution structural studies of rhodopsin and other GPCRs will form the basis to elucidate the detailed molecular mechanism of GPCR-mediated signal transduction.

CONTENTS

INTRODUCTION

Rhodopsin (Rho) is a highly specialized G protein–coupled receptor (GPCR) that detects photons in the rod photoreceptor cell. Within the superfamily of GPCRs that couple to heterotrimeric G proteins, Rho defines the so-called Family A GPCRs, which share primary structural homology (192, 207). Rho can be obtained from bovine retinae (0.5–1.0 mg/retina) by a sucrose density gradient centrifugation preparation of the rod outer-segment disc membranes (175). Rho is stable enough in the dark to be purified further by various chromatographic procedures, and it remains stable in solution in a variety of detergents (168). Bovine Rho was the first GPCR to be sequenced by amino acid sequencing (84, 171), the first to be cloned (157, 158), the first to be crystallized (167), and the first to yield a crystal structure (172).

Visual pigments share several structural features with other GPCRs (193). Their core structure consists of seven transmembrane (TM) segments (H1 to H7) (Figure 1). A pair of highly conserved Cys residues is found on the extracellular surface of the receptor and forms a disulfide bond. A Glu(Asp)/Arg/Tyr(Trp) tripeptide sequence is found at the cytoplasmic border of H3. This sequence is conserved in Family A GPCRs and is involved in G protein interaction (59, 60).

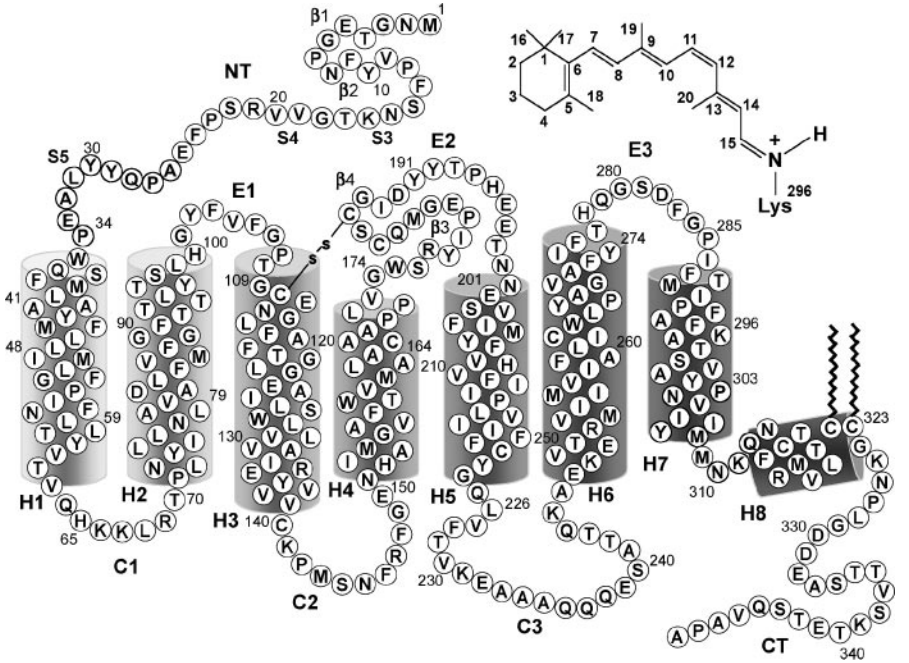

Figure 1 A secondary structure diagram of bovine Rho. Amino acid residues are depicted in single-letter code. The amino-terminal tail and extracellular domain is toward the top, and the carboxyl-terminal tail and cytoplasmic domain is toward the bottom. Transmembrane α-helical segments (H1 to H7) and the cationic amphipathic helix H8 are shown in cylinders. An essential disulfide bond links Cys-110 and Cys-187. Cys-322 and Cys-323 are palmitoylated. (*Inset*) The structure of the RET chromophore. Carbon atoms are numbered 1 through 20.

Sites of light-dependent phosphorylation at Ser and Thr residues are found at the carboxyl-terminal tail of most visual pigments. These sites are analogous to phosphorylation sites found on the carboxyl-terminal tails of other GPCRs (22).

Although it shares many similarities with other GPCRs, as a visual pigment Rho displays many specialized features not found in other GPCRs. In particular, visual pigments are made of opsin apoprotein plus chromophore. The chromophore is not a ligand in the classical sense because it is linked covalently via a protonated Schiff base bond in the membrane-embedded domain of the protein. The Lys residue that acts as the linkage site for the chromophore (Lys-296) is conserved within H7. A carboxylic acid residue that serves as the counterion to the protonated, positively charged retinylidene Schiff base (Glu-113) is conserved within H3. The position analogous to the Schiff base counterion is one helix turn away from the position of an Asp residue conserved in biogenic amine receptors that serves as the counterion to the cationic amine ligands.

The chromophore in all Rhos is derived from the aldehyde of vitamin A_1, 11-*cis*-retinal (RET) (Figure 1). Some fishes, amphibians, reptiles, and aquatic mammals may also employ the aldehyde of vitamin A_2, 11-*cis*-3,4-didehydroretinal, which contains an additional carbon-carbon double bond. All pigments with a vitamin A_2–derived chromophore are called porphyropsins. An important structural feature of the RET chromophore in Rho, in addition to its Schiff base linkage, is its extended polyene structure, which accounts for its visible absorption properties and allows for resonance structures (183).

Rho displays a broad visible absorption maximum (λ_{max}) at about 500 nm (Figure 2). Photon capture leading to photoisomerization of the 11-*cis* to all-*trans* form of the RET chromophore is the primary event in visual signal transduction, and it is the only light-dependent step (223). After photoisomerization, the pigment decays thermally to metarhodopsin II (M-II) with a λ_{max} value of 380 nm. The M-II intermediate is characterized by a deprotonated Schiff base chromophore linkage. M-II is the active form of the receptor (R^*), which catalyzes guanine nucleotide exchange by the rod cell heterotrimeric G protein, transducin (G_t). In contrast with vertebrate vision, invertebrate vision is generally photochromic—a photoactivated invertebrate pigment can be inactivated by absorption of a second photon that induces isomerization to the ground-state *cis* conformation.

In the case of the vertebrate visual system, G_t activation leads to the activation of a cyclic-GMP phosphodiesterase (cGMP-PDE) and the closing of cGMP-gated cation channels in the plasma membrane of the rod cell. Light causes a graded hyperpolarization of the photoreceptor cell. The amplification, modulation, and regulation of the light response is of great physiological importance and has been discussed in detail elsewhere (15, 32, 211, 223). Activation of a single Rho molecule by a single photon has been estimated to prevent the entry of as many as 10^7 cations into the rod cell. Recent studies have estimated that at room temperature, each R^* triggers activation of cGMP-PDE at rates of 1000 to 2000 molecules per second (120). Despite the fact that the visual system functions over about a 10^6-fold range of light intensity, the retinal rod cell has single-photon detection capability due to extremely low levels of dark noise in Rho and a significant degree of biochemical amplification. Thermal isomerization in a single Rho molecule at physiological temperature has been estimated to occur about once in 470 years (14). The possibility of single-pheromone molecule detection by insect olfactory systems notwithstanding, the visual system is unique among sensory signal transduction systems in that it can detect single events.

This review focuses on what has been learned from the recently published crystal structure of Rho (172). What insight does the structure provide about the mechanism of the "opsin shift" and spectral tuning? What is the structural basis for the incredible stability of Rho in the rod cell disc membrane in the dark? How does Rho achieve high photochemical specificity and high quantum yield? How does a single R^* catalyze guanine nucleotide exchange by hundreds of G_t molecules? What does the Rho structure tell us about structure-activity relationships in other GPCRs (148, 194)? Finally, when possible, attempts are made to reconcile previous key findings from biochemical studies and the analysis of site-directed mutant

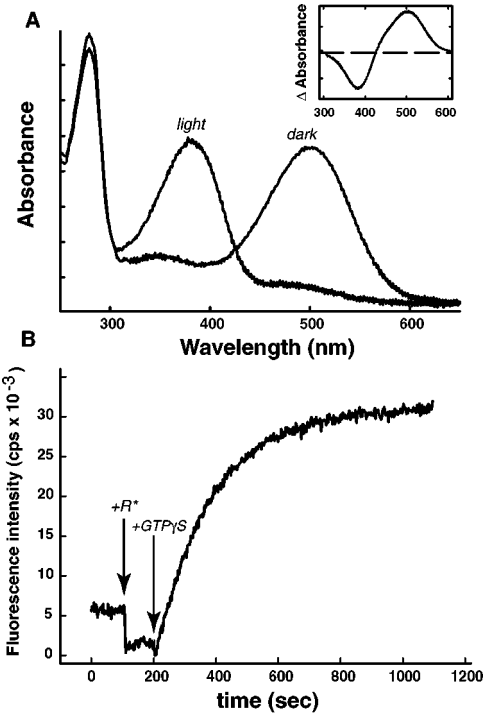

Figure 2 (*A*) A UV-visible absorption spectrum of purified recombinant COS-cell Rho in detergent solution (*dark*) shows a characteristic broad visible absorbance with a λ_{max} value of 500 nm. The 280-nm peak represents the protein component. After exposure to light, the pigment is converted to metarhodopsin II (M-II) with a λ_{max} value of 380 nm characteristic of an unprotonated Schiff base imine. M-II is the active form of the receptor that interacts with G_t. *Inset*: The photobleaching difference spectrum obtained by subtracting the light spectrum from the dark spectrum. Essentially identical results can be obtained with Rho from bovine retinas purified by concanavalin-A lectin-affinity chromatography. (*B*) A kinetic assay of the activation of G_t by R^*. The intrinsic tryptophan fluorescence of G_t increases significantly when GTP replaces GDP. Therefore, the fluorescence emission of a mixture of purified components (Rho, G_t, GDP, GTPγS) in detergent solution can be measured as a function of time. The sample is illuminated to convert Rho to R^*, which catalyzes GTPγS uptake by G_t and causes an increase in fluorescence. The reaction is started by injecting GTPγS into the cuvette (200 sec).

pigments with the Rho crystal structure. Some of the material herein has been presented in the context of the physiology rather than the biophysics of Rho, although there is obvious overlap (149). In addition, excellent recent reviews by Gether (69) and Ballesteros et al. (13) have focused more on the implications of the structure of Rho for understanding the structure and function of other GPCRs.

MOLECULAR STRUCTURE OF RHODOPSIN

Overview of the Crystal Structure of Rhodopsin

To obtain crystals, bovine Rho was purified from rod outer-segment membranes and crystallized from a detergent solution—nonylthiolglucoside supplemented with the small amphiphile heptane 1,2,3-triol (167, 168). The resolution of the crystallographic data of the original data set was approximately 2.8 Å, but small segments of the cytoplasmic surface domain are not resolved. A more recent refinement of the data has also been reported (218). The structure represents the inactive form of Rho with its bound RET chromophore intact. A ribbon diagram of the Rho peptide backbone structure with the RET chromophore is presented in Figure 3. The structure discussed in this chapter is that of the A chain in the

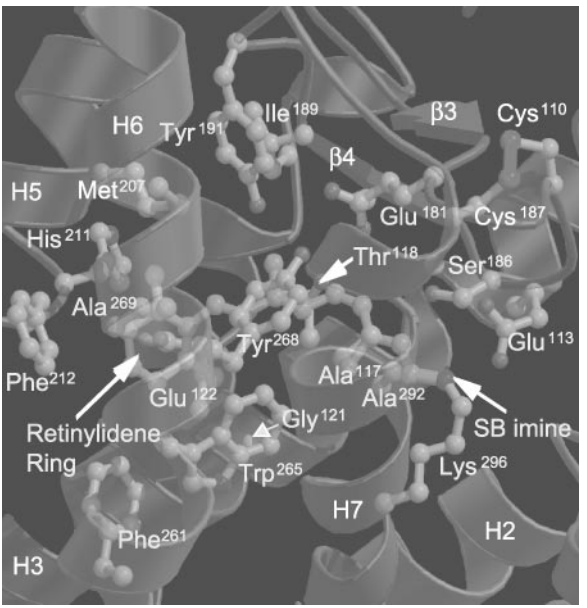

Figure 3 The RET chromophore-binding pocket of bovine Rho. The RET chromophore-binding pocket is shown from within the plane of the membrane bilayer. The cyclohexenyl ring and the Schiff base imine are labeled. At least 16 amino acid residues are within 4.5 Å of the RET ligand: Glu-113, Ala-117, Thr-118, Gly-121, Glu-122, Glu-181, Ser-186, Tyr-191, Met-207, His-211, Phe-212, Phe-261, Trp-265, Tyr-268, Ala-269, and Ala-292. Some additional key amino acid residues are labeled, including the Cys-110/Cys-187 disulfide bond. RET is situated such that its proximal end (approximately C_9 to C_{15}) lies along the β4 strand and its distal end (approximately C_9 to the cyclohexenyl ring) lies along H-3.

crystal unit cell dimer. A detailed description of the crystal structure was recently presented (149).

As an integral membrane protein, Rho comprises three topological domains: the extracellular surface, the membrane-embedded domain, and the intracellular surface. Due to the location of Rho in the disc membrane of the rod outer segment, the extracellular domain is sometimes referred to as intradiscal. The amino terminus of Rho is extracellular and the carboxyl terminus in intracellular. The membrane-embedded domain consists of seven TM segments (H1 to H7), which are predominantly α-helical. The helical segments form a compact bundle that contains the binding site for the RET chromophore.

Crystal Structure of the Extracellular Surface Domain of Rhodopsin

The extracellular surface domain of Rho comprises the amino-terminal tail (NT) and three interhelical loops (E1, E2, and E3) (Figure 1). There is significant secondary structure in the extracellular domain and several intra- and interdomain interactions. NT extends from the amino terminus to Pro-34 and contains five distorted strands (β1, β2, S3, S4, and S5). NT is glycosylated at Asn-2 and Asn-15. The oligosaccharides extend away from the extracellular domain and do not seem to interact with any part of the molecule. The extracellular surface domain also contains three extracellular interhelical loops: loop E1 (a.a. 101–106) connects H2 and H3, loop E2 (a.a. 174–199) connects H4 and H5, loop E3 (a.a. 278–285) connects H6 and H7.

One of the most striking features of the Rho structure is the presence and positioning of the β4 strand (Ser-186/Cys-187/Gly-188/Ile-189), which forms an extracellular roof for the RET-binding pocket. The β4 strand runs nearly parallel to the length of the polyene chain from about C_9 to the Schiff base imine nitrogen. The opposite end of RET from the cyclohexenyl ring to about C_{10} runs along H3, which is tilted with respect to the plane of the membrane. The result is that this end of RET seems to be held very firmly in place by multiple contacts.

Crystal Structure of the Membrane-Embedded Domain of Rhodopsin

The crystal structure of Rho suggests that 194 amino acid residues make up the seven TM segments (H1 to H7) included in the membrane-embedded domain: H1 (a.a. 35–64), H2 (a.a. 71–100), H3 (a.a. 107–139), H4 (a.a. 151–173), H5 (a.a. 200–225), H6 (a.a. 247–277), and H7 (a.a. 286–306). The crystal structure of this domain is remarkable for a number of kinks and distortions of the individual TM segments, which are otherwise generally α-helical in secondary structure. Many of these distortions from canonical secondary structure were not accounted for in molecular graphics models of Rho based on projection density maps obtained from cryoelectron microscopy (12, 119, 199, 219).

Crystal Structure of the Chromophore-Binding Pocket of Rhodopsin

The binding site of the RET chromophore lies within the membrane-embedded domain of the receptor (Figure 3). At least 16 amino acid residues are within 4.5 Å of the RET moiety: Glu-113, Ala-117, Thr-118, Gly-121, Glu-122, Glu-181, Ser-186, Tyr-191, Met-207, His-211, Phe-212, Phe-261, Trp-265, Tyr-268, Ala-269, and Ala-292. The most striking feature of the RET-binding pocket is the presence of many polar or polarizable groups to coordinate an essentially hydrophobic ligand (Figure 3). The chromophore is located closer to the extracellular side of the TM domain of the receptor than to the cytoplasmic side. The chromophore polyene from C_6 to C_{11} runs almost parallel to H3, which provides many of the amino acid side chains that form the chromophore-binding pocket: Glu-113, Gly-114, Ala-117, Thr-118, Gly-120, and Gly-121. The polyene chain facing toward the extracellular side of the receptor is covered, or capped, by the amino acid residues from the β4-sheet (Ser-186 to Ile-189) of the E2 loop as described above. The carboxylic acid side chain of Glu-181 in the β3-sheet of the E2 loop points toward the center of the RET polyene chain.

Glu-113 serves as the RET Schiff base counterion. A number of other amino acid side chains surround the imine moiety, including Tyr-43, Met-44 and Leu-47 in H1, Thr-94 in H2, and Phe-293 in H7. In particular, Met-44 and Leu-47, in addition to the peptide bond between Phe-293 and Phe-294, help to orient the side chain of Lys-296 in the direction of the long axis of Rho. The phenyl rings of Phe-293 and Phe-294 also interact with side chains of adjacent helices. The two oxygen atoms of the Glu-113 carboxylate side chain of Glu-113 are located 3.3 Å and 3.5 Å from the imine nitrogen. The hydroxyl group of Thr-94 is also about 3.4 Å from one of the Glu-113 carboxylate oxygens. Thr-92 and Thr-93 are also in the vicinity of the Schiff base imine but may not be close enough to contribute significantly to stabilization of its protonated ground state. The presence of water molecules in the Schiff base region has been postulated, but the crystal structure at the reported resolution does not contain defined water in this region (153).

The position of the cyclohexenyl ring of the chromophore is largely constrained on the cytoplasmic side of the binding pocket by three residues: Glu-122 (H3), Phe-261 (H6), and Trp-265 (H6). The indole side chain of Trp-265 points inward from the more cytoplasmic position of the Trp-265 backbone and comes within about 3.8 Å of the RET C_{20}. Side chains from Met-207, His-211, and Phe-212 on H5, and Tyr-268 and Ala-269 on H6 further constrain the chromophore ring.

Gly-121 interacts with RET in a direct steric manner and lies closest to the C_{18}-methyl group bonded to C_5 of the cyclohexenyl ring (Gly-121 C_α-RET C_{18} distance—3.5 Å). Gly-121 is close to Phe-261 (H6) in the Rho crystal structure. They pair to form one boundary of the RET-binding site, defining the C_4-C_5-C_{18} orientation (Phe-261 C_z-Gly-121 C_α distance, 5 Å; Phe-261 C_z-RET C_4 distance, 3.7 Å). This portion of the RET-binding pocket around H3 and H6 appears to be

held rigidly together by tight van der Waals interactions. H4 contributes only one residue, Cys-167, directly to the chromophore-binding pocket.

Crystal Structure of the Cytoplasmic Surface Domain of Rhodopsin

The cytoplasmic domain of Rho comprises three cytoplasmic loops and the carboxyl-terminal tail: C1 (a.a. 65–70), C2 (a.a. 140–150), C3 (a.a. 226–246), and CT (a.a. 307–348). Loops C1 and C2 are resolved in the crystal structure, but only residues 226 to 235 and 240 to 246 are resolved in C3. CT is divided into two structural domains. C4 extends from the cytoplasmic end of H7 at Ile-307 to Gly-324, just beyond two vicinal Cys residues (Cys-322 and Cys-323), which are posttranslationally palmitoylated. The remainder of CT extends from Lys-325 to the carboxyl terminus of Rho at Ala-348. The crystal structure does not resolve residues 328 to 333 in CT.

The hallmark of the C4 loop is an α-helical stretch, H8. H8 is connected to H7 by the Met-309/Asn-310/Lys-311 tripeptide that acts as a short linker. H8 lies nearly perpendicular to H7, and together with the Asn/Pro/X/X/Tyr motif in H7, it is one of the most highly conserved long stretches of primary structure in Rho. The environment around H8 is mainly hydrophobic, which may lead to increased helical stability. H8 might be best described as a cationic amphipathic α-helix, with Lys-311 and Arg-314 on one face of the helix and Phe-313, Met-317, and Leu-321 buried in the hydrophobic core of the bilayer between H1 and H7. H8 points away from the center of Rho and it appears that the palmitoyl groups linked to Cys-322 and Cys-323 by thioester bonds may be anchored in the membrane bilayer, although this is not resolved in the crystal structure. The helical structure of H8 is terminated by Gly-324. The residues at the extreme carboxyl-terminal end of CT compose the most solvent-exposed region of Rho. CT folds back over a small portion of the helical bundle at H1 and H7.

STRUCTURE-ACTIVITY RELATIONSHIPS IN RHODOPSIN

Structure-Activity Relationships in the Extracellular Surface Domain

The extracellular loops and amino-terminal tail of bovine Rho have been shown in a deletion analysis to be important for proper folding of the receptor that allows cellular processing and chromophore binding (42). Insertional mutagenesis was also used in a related study to probe the topology of Rho and to correlate the location of epitope insertion to stability and cell trafficking (27). Interestingly, several mutations that interfered with the formation of a correct tertiary structure on the intradiscal surface resulted in mutant opsins that appeared to be retained in the endoplasmic reticulum during heterologous expression and were complexed with molecular chaperones (9). Antibody accessibility studies suggested that the

NT domain constitutes a defined tertiary structure that contributes to the overall extracellular domain (31). Rho is glycosylated at Asn-2 and Asn-15 of the NT. A nonglycosylated Rho, which was prepared in the presence of tunicamycin, was defective in light-dependent activation of G_t (104). The structural basis of this finding is not clear from the Rho crystal structure because the oligosaccharide chains point away from the molecule and do not seem to engage in intramolecular interactions.

Several point mutations that result in amino acid substitutions in the NT domain are linked to autosomal dominant retinitis pigmentosa (ADRP), including positions Pro-23 and Gln-28. ADRP is an inherited human disease that causes progressive retinal degeneration, loss of dim-light vision, loss of peripheral vision, and eventual blindness. Pro-23 and Gln-28 interact with Tyr-102, which is in the E1 loop. This interaction might maintain an essential structural orientation between NT and E1 that is disrupted in the NT of the ADRP mutants. Thus, Tyr-102 interacts with Pro-23 and Gln-28 to maintain proper orientation between E1 and NT. The roles of specific amino acid residues in the NT domain were also studied in various transgenic mice strains harboring point mutations that correspond to sites linked to ADRP (149).

Cys-110 and Cys-187 form a disulfide linkage in an elegant study in which the four intracellular and three membrane-embedded Cys residues were removed by site-directed mutagenesis to create a mutant receptor with only the three extracellular Cys residues remaining (102). In a related study, the double mutant C110A/C187A was shown to bind RET to form a Rho-like pigment (39). However, the M-II–like photoproduct of the mutant pigment, which could activate G_t in response to light, was considerably less stable than native M-II (39).

Glu-181 arises from the linker between $\beta 3$ and $\beta 4$ and points toward the polyene chain. Glu-181 may serve to influence the electron density of the conjugated polyene system of the retinal chromophore so that photoisomerization occurs exclusively at the C_{11}-C_{12} double bond. Another potential role for Glu-181 may be to control the rate of decay of M-II. Recent experiments with site-directed mutants with replacements of Glu-181 show that the rate of M-II decay as measured by the decay of Trp fluorescence quenching can be either accelerated or slowed when the amino acid at position 181 is changed (M. Kazmi, S. De, E. Marin, E. Yan, R. A. Mathies & T. P. Sakmar, manuscript in preparation).

Structure-Activity Relationships in the Membrane-Embedded Domain of Rhodopsin

The membrane-embedded domain of Rho is characterized by the presence of several intramolecular interactions that may be important in stabilizing the ground-state structure of the receptor. One of the hallmarks of the molecular physiology of Rho is that it is essentially biochemically silent in the dark. The RET chromophore serves as a potent pharmacological inverse agonist to minimize activity. The result is that the rod cell can attain single-photon sensitivity (86). The Rho structure reveals numerous potentially stabilizing intramolecular interactions—some

mediated by the RET chromophore and some arising mainly from interhelical interactions that do not involve the RET-binding pocket directly. For example, Phe-293 interacts with Leu-40 and Phe-294 interacts with Cys-264. These interactions seem to be facilitated by the slight distortion of H6 in the region near Ile-263. In addition to these core interactions, four hydrogen (H)-bond networks appear to provide stabilizing interhelical interactions at or near the cytoplasmic surface of the receptor.

H-bond network 1 links H1, H2, and H7. The helical structure of H7 is elongated in the region from Ala-295 to Tyr-301, which permits the backbone carbonyl group of Ala-299 to H-bond with the side chains of Asn-55 and Asp-83. Asn-55 is a highly conserved residue that plays the central role in the H-bond network 1 because it H-bonds to both Asp-83 and the backbone carbonyl of Ala-299. Asp-83 may be connected to the backbone carbonyl of Gly-120 in H3 through a water molecule.

H-bond network 2 links H2, H3, and H4. This network involves Asn-78 as the key residue, which H-bonds to the hydroxyl functions of Ser-127 (H3), Thr-160 (H4), Trp-161 (H4), and the backbone carbonyl of Phe-159. Mutant pigments S127A and T160V displayed normal ground-state spectral properties consistent with a lack of direct contact with RET (96). Another possible interhelical interaction in this region might involve Glu-122 (H3), Met-163 (H4), and His-211 (H5). An indirect functional interaction between Glu-122 and His-211 has been demonstrated experimentally (18).

H-bond network 3 links H3 and H6. This network involves the conserved Arg-135, which interacts with Glu-134 and with the hydroxyl group of Thr-251 and side chain of Glu-247. The carboxylate of Glu-134 seems to be in position to form a salt bridge with the guanidinium group of Arg-135. This would be consistent with the hypothesis that Glu-134 is unprotonated in Rho and becomes protonated during the transition to R^* (10, 50). It is interesting to note the three consecutive Val residues (Val-137, Val-138, and Val-139) are situated to form a cytoplasmic cap to H3 so that the Glu-134/Arg-135 dipeptide is between the receptor core and the Val tripeptide. This Val cap might act to stabilize the Glu-134/Arg-135 salt bridge, which in turn acts to keep the receptor in its off-state in the dark. It is also interesting to note that Thr-251 in Rho is in the position equivalent to Ala-293 in the α_{1B}-adrenergic receptor. Mutation of Ala-293 causes the receptor to become constitutively active (112). The Asp(Glu)/Arg/Tyr(Trp) motif at the cytoplasmic border of H3 is one of the most highly conserved structural motifs in Family A GPCRs.

Finally, H-bond network 4 links H6 and H7. The key interaction here is between Met-257 and Asn-302. The precise functional importance of the highly conserved Asn/Pro/X/X/Tyr motif (Asn-302/Pro-303/Val-304/Ile-305/Tyr-306 in Rho) is unclear. However, one key structural role is to mediate several interhelical interactions. The side chains of Asn-302 and Tyr-306 project toward the center of the helical bundle. The hydroxyl group of Tyr-306 is close to Asn-73 (cytoplasmic border of H2), which is also highly conserved. A key structural water molecule may facilitate a H-bond interaction between Asn-302 and Asp-83 (H2). A recent mutagenesis study of the human platelet-activating factor receptor showed that replacement of amino acids at the positions equivalent to Asp-78 and Asn-302 in

Rho with residues that could not H-bond prevented agonist-dependent receptor internalization and G protein activation (125).

The interaction between Met-257 and the Asn/Pro/X/X/Tyr motif was predicted earlier to explain the results of a mutagenesis study in which Met-257 was replaced by each of the 19 other amino acid residues (82). Nearly all Met-257 replacements caused constitutive activity of the mutant opsins. Constitutive activity refers to the ability of an opsin to activate G_t in the absence of any chromophore. A decrease in interaction between Met-257 and Asn-302 might relieve an interhelical constraint that stabilizes the ground-state structure of Rho. However, the most highly constitutively active Met-257 mutants were M257Y, M257N, and M257S, which are all theoretically capable of forming H-bonds with the adjacent Asn-302. It is conceivable that the amino acid residue at position 257 in a mutant receptor forms H-bond interactions that stabilize the active-state structure of the receptor as well. Whether constitutive activity is caused simply by a lack of H6/H7 interactions, or whether a gain of active-state stabilizing interactions is required could be determined by testing mutant receptors with alterations of the Asn/Pro/X/X/Tyr motif, for example, N302A and I305A in Rho, or analogous mutations in other Family A GPCRs.

Structure-Activity Relationships in the Chromophore-Binding Pocket of Rhodopsin

The RET chromophore is a derivative of vitamin A_1 with a total of 20 carbon atoms (Figure 1). The carbon atoms of the cyclohexenyl ring are numbered C_1 to C_6. The polyene carbons extend from C_7 to C_{15}. Two methyl groups (C_{16} and C_{17}) are bonded to C_1, and single methyl groups are attached at each of three other carbons: C_5 (C_{18} methyl), C_9 (C_{19} methyl), and C_{13} (C_{20} methyl). The structural conformation of the bound chromophore in the Rho crystal structure appears to be 6-s-*cis*, 11-*cis*, 12-s-*trans*. The protonated Schiff base bond appears to be in the *anti* conformation. A higher-resolution Rho structure would be required for a crystallographic determination of the precise chromophore structure. Although a variety of spectroscopic studies support the 6-s-*cis*, 11-*cis*, 12-s-*trans* RET conformation, recent NMR and computational experiments suggest a 6-s-*trans* conformation (74, 202).

A number of experimental approaches have been employed to investigate RET-protein interactions in the membrane-embedded domain of bovine Rho. Several spectroscopic methods such as resonance Raman spectroscopy (93, 117, 129), Fourier-transform infrared (FTIR)-difference spectroscopy (51) and NMR spectroscopy (44, 74, 75, 221) have been reported. Other approaches have included reconstitution of opsin apoprotein with synthetic retinal analogues (92, 137) and photochemical cross-linking (26, 154, 232).

Lys-296 and Glu-113 are two of the key amino acid residues that define the structure and function of the retinal chromophore in Rho. The Schiff base linkage of the chromophore to Lys-296 is a key feature of Rho structure (83). Light-dependent Schiff base deprotonation is required for the formation of the active state of the receptor, R^* (106, 136). However, light can induce the receptor active state in the absence of a Schiff base chromophore linkage to the opsin (169, 234).

Glu-113 in bovine Rho serves as the counterion to the positive charge of the RET-protonated Schiff base (49, 156, 196, 233). Glu-113 is unprotonated and negatively charged in the ground state of Rho (48). It becomes protonated upon light-dependent formation of M-II and is the net proton acceptor for the Schiff base proton (97). The Glu-113–protonated Schiff base interaction serves to stabilize the Schiff base proton such that its acid dissociation constant (pK_a) in Rho is estimated to be >12, compared to a value of ~7 for a model compound in aqueous solution, although the mechanism of protonated Schiff base stabilization is not entirely clear from the crystal structure. The stable interaction between Glu-113 and the protonated Schiff base may also inhibit hydrolysis of the Schiff base linkage in darkness. For example, hydroxylamine does not react with the Schiff base of Rho, but readily reacts with that of M-II or with Rho mutants in which Glu-113 is replaced by a neutral amino acid residue by mutagenesis (196). This is an important consideration since the opsin alone, without the RET chromophore, has a small but measurable activity (29, 183, 189, 215).

The chemical environment of Schiff base has recently been probed using magic angle spinning (MAS) NMR. Recombinant Rho was labeled with 6-^{15}N-lysine and 2-^{13}C-glycine by expression of opsin in tissue culture with defined media. The UV-visible spectrum of the labeled Rho was indistinguishable from that of wild-type Rho. The peak corresponding to the ^{15}N-PSB was observed at 156.8 ppm in the MAS NMR spectrum. This peak position suggests that the distance between the PSB and its counterion at Glu-113 is greater than 4 Å, consistent with structural H-bonded water between the PSB nitrogen and Glu-113 (44). Similar results were obtained by Creemers et al. (38). More recently MAS NMR was carried out on artificial rhodopsin prepared by regeneration of opsin with a synthetic retinal containing ^{13}C at ten positions (222).

The high sensitivity of the rod cell depends upon an extremely low intrinsic level of signaling in darkness. Dark noise can be generated by thermal isomerization events in Rho (16, 17, 229), by the presence of opsin lacking the RET chromophore, which acts as an inverse agonist, or by mutant opsins that display the property of constitutive activity (189). Generally, a mutation that disrupts a putative salt bridge between Glu-113 and Lys-296 in the opsin apoprotein leads to constitutive activity. Replacement of either Glu-113 or Lys-296 by a neutral amino acid results in a mutant opsin with constitutive activity.

Other mutations such as G90D or A292E also result in constitutive activity, presumably because the introduction of the negatively charged residue into the membrane-embedded domain of the receptor affects the stability of the Glu-113/Lys-296 salt bridge (36, 184). The crystal structure shows that H2 is kinked around vicinal Gly residues, Gly-89 and Gly-90, so that this region of H2 is brought closer to H3 than to H1. This feature is interesting in that Gly-90 comes into close proximity to the retinylidene Schiff base counterion, Glu-113, on H3. A mutation that results in the replacement of Gly-90 by an Asp residue causes congenital stationary night blindness in humans, probably because of destabilization of the ionic interaction between Glu-113 and the Schiff base (235), or because of constitutive activity of the mutant opsin apoprotein that results from a disruption of a salt bridge

between Glu-113 and Lys-296 (184). The mechanism of constitutive activity of opsins and the potential relevance of constitutive activity to visual diseases such as congenital night blindness have been reviewed (185).

The C_{12} of RET is within about 4–5 Å of Glu-181 from the E2 loop. Glu-181 may serve to influence the electron density of the conjugated polyene system of the RET chromophore so that photoisomerization occurs exclusively at the C_{11}–C_{12} double bond. The potential for ionic interaction between RET and Glu-181 also suggests that it may have a role in the mechanism of the opsin shift. Perturbation of the electron distribution near the center of the polyene chain is one mechanism to facilitate spectral tuning (92). Glu-181 is highly conserved among vertebrate opsins, blue and UV cone pigments. The corresponding position in green and red cone pigments is His-197, which forms part of a chloride ion–binding site. Chloride binding causes a red shift in absorption of the green and red pigments. Interestingly, the H197E/R200Q mutant of the human green cone pigment displays a visible λ_{max} value of 500 nm (225), which is the same as the λ_{max} value of Rho, suggesting that perturbation of the polyene by chloride may be the only element in the green cone pigment responsible for its spectral difference from Rho. The negative charge of the chloride ion bound to His-197 in the long-wavelength-sensing cone pigments might be brought closer to RET than the charge of the carboxylate of Glu-181 in Rho.

The position of the cyclohexenyl ring of the chromophore is largely constrained on the cytoplasmic side of the binding pocket by three residues: Glu-122 (H3), Phe-261 (H6), and Trp-265 (H6). The indole side chain of Trp-265 points inward from the more cytoplasmic position of the Trp-265 backbone and comes within about 3.8 Å of the RET C_{20}. Trp-265 is close enough to RET that it can serve as an intrinsic probe of the chromophore conformation (130). Side chains from Met-207, His-211, and Phe-212 on H5, and Tyr-268 and Ala-269 on H6 further constrain the chromophore ring. Replacements of Phe-261 by Tyr or Ala-269 by Thr produce bathochromic spectral shifts in the λ_{max} values of the resulting mutant pigments (34). These residues are also responsible in part for the spectral shift in red cone pigments. Whereas red pigments have Thr and Tyr at the positions corresponding to 261 and 269 in Rho, green cone pigments have Phe and Ala (11, 161).

The interaction between Gly-121 and RET is consistent with mutagenesis experiments in which replacement of Gly-121 caused blue-shifted λ_{max} values and decreased RET binding that corresponded to the bulk of the substituted side chain (80). Second-site replacement of Phe-261 by Ala caused a reversion of the loss of function Gly-121 mutant phenotypes, which was interpreted to mean that Gly-121 and Phe-261 interacted to form a part of the RET-binding pocket (79). Gly-121 and Phe-261 are indeed very close together in the Rho crystal structure. They pair to form one boundary of the RET-binding site to define the C_4-C_5-C_{18} orientation (Phe-261 C_z-Gly-121 C_α distance, 5 Å; Phe-261 C_z-RET C_4 distance, 3.7 Å). Interestingly, Gly-121 is conserved among all vertebrate and invertebrate visual pigments (181), and Phe-261 is strictly conserved among nearly all GPCRs (5). In long-wavelength-sensing cone pigments, Phe-261 is replaced by a tyrosine that is involved in spectral tuning (34).

Structure-Activity Relationships in the Cytoplasmic Domain of Rhodopsin

A number of cytoplasmic proteins interact exclusively with R*. Because the crystal structure depicts the inactive Rho structure that does not interact significantly with cytoplasmic proteins, the structure can provide only indirect information about the relevant R* state. In addition, two regions of the cytoplasmic surface domain of Rho (amino acid residues 236–239 and 328–333) are not fully resolved in the crystal structure. Potentially important structural information relevant to understanding protein-protein interactions in the visual transduction cascade may be lacking in the reported structure. The borders between the TM helical segments and the cytoplasmic loops do not necessarily represent the boundary between aqueous phase and membrane bilayer. The helical segments generally tend to extend into the cytoplasmic aqueous phase. A number of amino acid residues that are involved in G_t binding or activation, such as Glu-134 or Lys-248, are situated in the helical segments.

Detailed biochemical and biophysical analysis of the R*-G_t interaction has been aided by mutagenesis of the cytoplasmic domain of bovine Rho. Numerous Rho mutants defective in the ability to activate G_t have been identified (60). Several of these mutant receptors were studied by flash photolysis (46, 59), light scattering (45), or proton uptake assays (10). Recently, a combination of site-directed mutagenesis and peptide-binding studies clearly showed that the C4 loop region, which includes H8, is involved in G_t binding and activation (46, 143). Direct evidence for the interaction between H8 and G_t comes from studies using a synthetic peptide corresponding to Asn-310 to Leu-321 of Rho, which binds to G_t (143). The key overall result of these studies is that C2, C3, and H8 are involved in R*-G_t interaction.

H8 is a cationic amphipathic helix that may bind a phospholipid molecule, especially a negatively charged phospholipid such as phosphatidyl serine. In fact, spectroscopic evidence has been reported to show an interaction between Rho and a lipid molecule that is altered in the transition of Rho to M-II (19, 96). High conservation of Phe-313 and Arg-314 suggests that the amphipathic character of H8 may be functionally important. H8 points away from the center of Rho, and the area of the membrane surface covered by the entire cytoplasmic surface domain appears to be roughly large enough to accommodate G_t in a one-to-one complex. Recent evidence from fluorescence anisotropy and circular dichroism spectroscopy suggests that the structure of H8 is highly dependent on environment. Specifically, peptides corresponding to H8 adopt a random coil configuration in aqueous solution but form α-helices upon exposure to sodium dodecyl sulfate or binding to phospholipid liposomes (A. G. Krishna, T. J. Tracy, S. T. Menon & T. P. Sakmar, manuscript in preparation). The CT distal to the palmitoylated Cys-322 and Cys-323 residues appears to be highly disordered and dynamic based upon the results of site-directed electron paramagnetic resonance (EPR) spin labeling (124).

The structure of the cytoplasmic surface of Rho was also probed by solution ^{19}F nuclear Overhauser effect (NOE) NMR. NOE resonance depends on the distance between two atomic nuclei that undergo spin-spin coupling. To facilitate

NOE NMR in Rho, ^{19}F was introduced at specific sites in Rho using site-directed mutagenesis, which replaced the targeted amino acid with Cys. The Cys residue was then reacted with 4,4′-dithiodipyridine followed by trifluoroethylthio to yield a disulfide-linked trifluoroethyl moiety. As a control, individual Cys mutants were prepared in this manner to give the ^{19}F label at Cys-67, Cys-140, Cys-245, Cys-248, Cys-311, and Cys-316. Illumination of the individual mutants to form M-II produced upfield chemical shifts for the proteins labeled at positions 67 and 140, and downfield shifts for labels at positions 248 and 316. There was little or no change for proteins labeled at 245 and 311 (113). To allow the NOE strategy, three pairs of Cys residues were labeled in the same manner: Cys-140/Cys-316, Cys-65/Cys-316, and Cys-139/Cys-257. The labeled recombinant pigments were studied in the dark. No enhancement of the NOE signal was observed for the Cys-139/Cys-257 pair, moderate negative enhancement was observed for the Cys-65/Cys-316 pair, and strong negative enhancement was observed for the Cys-139/Cys-251 pair, indicating proximity of Cys-139 and Cys-251 (135).

THE MOLECULAR MECHANISM OF RECEPTOR ACTIVATION

Although the crystal structure of Rho does not provide direct information about the structure of R^* or about the dynamics of the Rho-to-R^* transition, it does provide a wealth of information that should help to design experiments using existing methods to address specific questions regarding the molecular mechanism of Rho activation. Fourier-transform infrared (FTIR)-difference spectroscopy has proven to be a well-suited technique for the study of light-induced conformational changes in recombinant Rho mutants (51, 190, 201). For example, among the membrane-embedded carboxylic acid groups, light-induced changes of protonation states or H-bond strengths were deduced from characteristic frequency shifts of C═O stretching vibrations of protonated carboxylic acid groups in FTIR-difference spectra. Their assignment to specific Asp or Glu residues was based on the disappearance of specific difference bands in site-directed mutants and revealed that Asp-83 (48, 186) and Glu-122 (48) are protonated in both dark Rho and M-II, whereas Glu-113 is ionized in the dark state and becomes protonated in M-II (97). Recently, attenuated total reflectance (ATR) FTIR-difference spectroscopy of the R^*-G_t (or peptides derived from G_t) complex revealed an infrared-difference band that could be assigned to protonation of Glu-134 (47, 52, 163).

Evidence for the importance of steric interactions distal to the Schiff base comes from FTIR studies using ring-modified retinal analogues. Increased flexibility, as in 5,6-dihydro (65) or 7,8-dihydro analogues (173), reduces the usually observed torsions along the retinal chain in the intermediate trapped at 80 K where bathorhodopsin would normally be stable. In addition, the protein conformational changes observed at temperatures that stabilize the metarhodopsin I (M-I) or M-II intermediates differ from those observed in native Rho. In an extreme case,

illumination of a pigment regenerated with a retinal analogue lacking the cyclohexenyl ring fails to induce the complete set of infrared absorption changes typical of the M-II conformation and results in reduced G_t activation (98). Therefore, the cyclohexenyl ring must transmit important steric changes to the protein. This model seems consistent with the location of the RET ring in the crystal structure of Rho.

Movement of α-helical domains is known to be involved in the signal transduction mechanisms of some TM receptor proteins, such as the bacterial chemoreceptors (150), and has been shown to occur during the proton-pumping cycle following retinal isomerization in bacteriorhodopsin (bR), the seven-transmembrane segment light-driven proton pump (212–214). Recent studies have suggested that steric and/or electrostatic changes in the ligand-binding pocket of Rho may cause changes in the relative disposition of TM helices within the core of the receptor. These changes may be responsible for transmitting a signal from the membrane-embedded–binding site to the cytoplasmic surface of the receptor. Trp mutagenesis (130), mutagenesis of conserved amino acid residues on H3 and H6 (79, 80), and the introduction of pairs of His residues at the cytoplasmic borders of TM helices to create sites for metal chelation (200) have recently provided insights regarding the functional role of specific helix-helix interactions in Rho.

The indole group of a Trp amino acid residue is often used as a noninvasive environment-sensitive probe of protein structure because of its unique absorption and fluorescence properties. UV-absorption spectroscopy has suggested that the local protein environment around Trp residues changes during the conversion of Rho to M-II (182). In addition, a linear dichroism study of UV-difference bands indicated a reorientation of an indole side chain during the M-I to M-II conversion (33). More specifically Trp-126 and Trp-265 were shown to move to more polar environments during activation of the receptor (130). It was further suggested that the photoactivation of Rho involved a change in the relative disposition of H3 and H6, which contain Trp-126 and Trp-265 within the α-helical bundle of the receptor.

The functional interaction of H3 and H6 was further probed in a study in which metal ion–binding sites were introduced between the cytoplasmic surfaces of TM helices with the aim of restraining specific activation-induced conformational changes (200). Pairs of His residues are capable of chelating metal ions such as Zn(II) if the distance and geometry between the residues are appropriate. His residues substituted for the native amino acids at the cytoplasmic ends of H3 and H6, but not H5 and H7, created mutant proteins that activated G_t in the absence, but not in the presence, of metal ions. It was concluded that specific metal ion cross-links between positions 138 and 251, or 141 and 251, on H3 and H6 prevented receptor activation. These results indicated a direct coupling of receptor activation to a change in the spatial disposition of H3 and H6. This could occur if movements of H3 and H6 were coupled to changes in the conformation of the connected intracellular loops, which contribute to binding surfaces and tertiary contacts of Rho with G_t (59, 60).

More evidence for changes in interhelical interactions upon receptor activation was provided by extensive site-directed spin labeling and EPR spectroscopy studies of the transition of Rho to R* in modified or expressed mutant pigments. The results suggested a requirement for rigid body motion of TM helices, especially H3 and H6, in the activation of Rho (55). A slight reorientation of helical segments upon receptor activation is also supported by experiments using polarized attenuated total reflectance infrared-difference spectroscopy (40). Finally, movement of H6 was also detected by site-specific chemical labeling and fluorescence spectroscopy (43). The structural rearrangement of helices upon activation might not result in a R* structure that is drastically different from that of Rho since an engineered receptor with four disulfide bonds (between the cytoplasmic ends of H1 and H7 and H3 and H5, and the extracellular ends of H3 and H4 and H5 and H6) was still able to activate G_t (209).

However, some conformational changes must occur at the cytoplasmic surface of Rho to produce R* that can activate G_t. Does the Rho structure provide any potential insights that might help to predict the identity of these conformational changes? Does H8 unwind or come off the membrane surface on activation? Do C2 and C3, which are known to be important for G_t activation, move? What are the active-state conformations of the conserved Glu-134/Arg-135/Tyr-136 in H3 and the conserved Asn-302/Pro-303/Val-304/Ile-305/Tyr-306 in H7?

Mutagenesis experiments can be designed to elucidate the light-dependent alterations of physical or chemical states of specific amino acids required for G_t activation. For example, structural changes in the cytoplasmic surface domain of Rho were suggested by changes in the reactivities of Cys residues introduced at various positions by site-directed mutagenesis (114). Conformation-dependent interhelical interactions and tertiary contacts on the cytoplasmic surface were also probed biochemically using site-directed disulfide bond formation (208) and/or expression of split receptors (230, 231). Using the core of Rho as a scaffold, cytoplasmic loops of other GPCRs were substituted for those of Rho, the results of G protein–activation experiments suggested that C2 and C3 might have distinct roles in G_t activation and G protein–subtype specificity (228). These results also indirectly support the general activation mechanism of helix movement that transmits a signal from the membrane-embedded core to the surface loops of the receptor.

Time-resolved (54) and static EPR spectroscopy studies (187) on site-specific spin-labeled Rho showed that the cytoplasmic terminations of H3 and H7 undergo structural rearrangements in the vicinities of Cys-140 and Cys-316. These changes have been specifically assigned to the M-II conformation. Cys-140 is close to the highly conserved Glu-134/Arg-135/Tyr-136 tripeptide at the cytoplasmic border of H3. Site-directed spin labeling of the amino acid residues from Tyr-306 to Leu-321 was also carried out. The information obtained regarding conformational changes in H8 upon M-II formation was limited by the relative lack of reactivity of the Cys residues engineered into positions 317, 318, 320, and 321. However, structural changes were detected at positions 306, 313, and 316, consistent with movements of the nearby H6 and with biochemical evidence for a light-dependent interaction

between Cys-65 and Cys-316 in native Rho (6, 30). Consistent with the notion of light-dependent structural changes in the vicinity of the cytoplasmic end of H7 is the observation that a monoclonal antibody with an epitope that was mapped to the amino acid sequence 304 to 311 bound only to R^* and not to Rho (1). Only relatively small light-dependent structural changes were noted in and around the C1 loop when residues 56 to 75 were individually probed by site-directed spin labeling (7).

An EPR study of Rho mutants with a substitution of Glu-134 showed that the mutant receptors displayed an EPR signature consistent with a partially activated conformational state in the dark (107). This finding seems to be consistent with extensive earlier studies of Glu-134 replacement mutants. The structural change detected by EPR spectroscopy may be directly related to the apparent requirement for protonation of Glu-134 upon R^* formation. A rearrangement of neighboring H-bonding partners may be necessary for protonation of Glu-134 to occur. The pH profile of G_t activation (50) as well as the abolishment of the uptake of two protons in mutant E134Q (10) suggests the existence of other titratable groups influenced by Glu-134. Glu-134 interacts primarily with Arg-135 in Rho, but it is not clear whether Glu-134 would interact with other side chains in R^* or simply be in a position to interact with bound G_t. The Glu-134/Arg-135 dipeptide may form a functional microdomain that is responsible for inducing the release of GDP from R^*-bound G_t (3, 128).

Any model of receptor activation has to account for the fact that the chemical environment of the Schiff base is altered so that net proton transfer occurs between the Schiff base imine and Glu-113 (97). This change in the RET-binding pocket must be transmitted to the cytoplasmic surface of the receptor. The Rho crystal structure is consistent with the helix movement model of receptor activation (55, 200) since it provides a structural basis to explain how chromophore isomerization could lead to displacement of H3 and H6 that would subsequently result in a change in orientation of Glu-134 at the cytoplasmic border. The structure suggests possible contacts between the cyclohexenyl ring of the chromophore and H3, which should change upon photoisomerization (26). At the Schiff base end of the chromophore, the C_{20} methyl group seems to interact with Trp-265, and this interaction should also change upon isomerization. Other key interhelical constraints are expected to be directly sensitive to chromophore isomerization, including those mediated by Phe-294, Ala-299, Asn-302, and Tyr-306. Any concerted disruption of stabilizing interhelical interactions may be expected to lead to helix movement and rearrangement of the helical bundle.

MECHANISM OF THE OPSIN SHIFT AND SPECTRAL TUNING

Rho has been used as a model pigment for a variety of chemical and spectroscopic studies to elucidate the mechanism of the opsin shift. In this context, the opsin shift may be defined as the difference between the λ_{max} value of a RET Schiff

base model compound (about 440 nm) in solution and that of Rho (500 nm). One important result to arise from the study of mutant bovine Rho pigments was the identification of Glu-113 as the RET Schiff base counterion (156, 196, 233). UV-visible spectroscopy (155, 156, 196, 233) and microprobe resonance Raman spectroscopy (132) were also used to characterize other membrane-embedded carboxylic acid residues. Additional studies including the use of photoaffinity reagents (154, 232), retinal analogues regenerated with site-directed mutants (188) or site-directed mutant pigments (79, 80, 130, 155), led to a more complete picture of the amino acid residues in the membrane-embedded domain of Rho that interact with the retinal chromophore.

Microprobe Raman spectroscopy of recombinant visual pigments and mutant pigments in particular has provided useful information about the mechanism of the opsin shift (132). Raman spectroscopy measures the energy loss of photons that are scattered after laser excitation of a nonabsorbing medium. The energy loss (expressed in wavenumbers) is proportional to the vibrational frequencies of the excited molecule. Conditions can be chosen such that a vibrational spectrum of the 11-*cis*-retinylidene chromophore can be obtained within its binding pocket in the Rho pigment. Vibrational modes are represented as peaks of Raman intensity. Some of the modes are delocalized. The in-phase ethylenic stretching mode at 1545 cm^{-1} represents the coupled vibrations of the conjugated carbon-carbon double bonds. Other modes are localized and represent specific atomic vibrations within the chromophore. The 1650 cm^{-1} mode represents the C=N stretching vibration of the protonated Schiff base. The 970 cm^{-1} mode represents the coupled hydrogen-out-of-plane (HOOP) wagging of C_{11}-H and C_{12}-H. The 1212 cm^{-1} mode represents the coupled C_8-C_9 stretching and C-H rocking motions. Other C-C stretching modes are represented by the 1098 (C_{10}-C_{11}), 1190 (C_{14}-C_{15}), and 1238 cm^{-1} (C_{12}-C_{13}) peaks. These modes can be used as probes of local structure and may be sensitive to specific amino acid replacements introduced by site-directed mutagenesis (116).

The crystal structure now provides a clear picture of the RET chromophore-binding pocket in Rho (Figure 3). Available data suggest that the dominant mechanism responsible for the opsin shift is the interaction of dipolar amino acid residues with both the ground-state and excited-state charge distributions of the chromophore (116, 131). This general mechanism is supported by the crystal structure in that the RET-binding pocket contains a large number of dipolar or polarizable amino acid residues.

THE RHODOPSIN PHOTOCYCLE

The chromophore photoisomerization occurs on an ultrafast timescale and was observed to be a vibrationally coherent process (224). At low temperature, a number of photointermediates that characterize the transition of Rho to R* can be trapped and studied by a variety of spectroscopic techniques. Laser flash photolysis coupled with nanosecond time-resolved UV-visible spectroscopy has identified the Rho

photocycle that occurs at or near physiological temperature: Rho (500 nm) → bathorhodopsin (543 nm) ↔ blue-shifted intermediate (BSI) (477 nm) → lumirhodopsin (497 nm) → M-I (480 nm) ↔ M-II (380 nm). M-II decays to metarhodopsin III (M-III) (450 nm) and finally to opsin plus free 11-*trans*-retinal (126).

The photointermediates of Rho and a variety of native visual pigments, chemically modified pigments, and artificial pigments have been studied by optical, resonance Raman, FTIR, and NMR spectroscopy (24, 48, 53, 57, 81, 113, 115, 127, 130, 132, 173, 180, 195, 201). These studies provide specific detailed information about chromophore structures and about dynamic chromophore-opsin interactions. The photocycle can also be studied under a variety of conditions that might provide a basis for identifying specific amino acid residues that might be involved in intramolecular proton transfer reactions. For example, the pH dependency was determined for the formation of Rho photoproducts from lumi to M-II (99).

THE STRUCTURAL BASIS OF RHODOPSIN-TRANSDUCIN INTERACTIONS

Structural Studies of Transducin

G_t plays a central role in the phototransduction cascade (210, 223). G_t couples together two separate highly specialized proteins: the photon detector rhodopsin and the efficient second messenger modulator PDE. G_t activation by R^* represents a key amplification step in the cascade in that a single R^* can catalyze the activation of hundreds of G_t molecules (63, 87). In addition, G_t exhibits a low rate of basal (uncatalyzed) nucleotide exchange that contributes to sensitivity by maintaining low background noise. Finally, G_t provides an important site of regulation. The rates of GTP loading and GTP hydrolysis by G_t determine to a large extent the amplitude and the temporal resolution of the resulting signal. Crystal structures of several conformations of G_t have been solved to date, including the GTPγS- (164), the GDP- (121), and the GDP/AlF_4^--bound structures of Gα_t (205), as well as the GDP-bound heterotrimer (122) and free G$\beta\gamma_t$ (204) (Table 1; follow the Supplemental Material link on the Annual Reviews homepage at http://www.annualreviews.org/). More recently, the structure of the ternary complex of Gα_t bound to its effector PDEγ and RGS9 was reported (203). These structures have provided detailed information on a number of G protein mechanisms, including the nature of the conformational change induced by GTP binding, the mechanism and regulation of GTP hydrolysis, and the nature of interactions between Gα_t and G$\beta\gamma_t$.

Gα_t, a 350–amino acid protein, consists of two domains (Figure 4)—the Ras-like domain, so named because of its homology with the structure of the monomeric G protein, $p21^{ras}$ (Ras), and the helical domain, so named to reflect its composition of six α-helices (αA-αF). The nucleotide is bound in a cleft between the domains. The Ras-like domain consists of a central mixed six-stranded β-sheet (designated β1-β6) surrounded on either side by a total of six α-helices (designated α1-α5, plus αG). The majority of the direct contacts to the nucleotide originate from conserved

regions of the Ras-like domain, which map to loops emanating from the strands of the central β-sheets. These loops are homologous to canonical nucleotide-binding domains of the monomeric G proteins (206). The Ras-like domain contains four regions not homologous to Ras, called Inserts 1–4.

The conformational changes that accompany the exchange of GDP for GTP are localized to three regions, denoted Switch I, II, and III. Switch I (Ser-173-Thr-183) and II (Phe-195-Thr-215) are similar to Switch regions described in Ras; Switch III (Asp-227-Arg-238) is unique to the heterotrimeric G proteins. Switch I and II respond directly to the presence of the γ phosphate of GTP, but Switch III appears to move in response to reorganization of the Switch II (121). The conformational changes in Switch II involve a partial rotation of the α2-helix, which leads to the movement of several amino acid side chains from exposed to partially buried positions. These changes serve as the basis of assays of $G\alpha_t$ activation. In particular, the movement of Trp-207 is detected as a large increase in fluorescence emission intensity (52, 56), and the burial of Arg-204 protects it from cleavage by trypsin (62, 141).

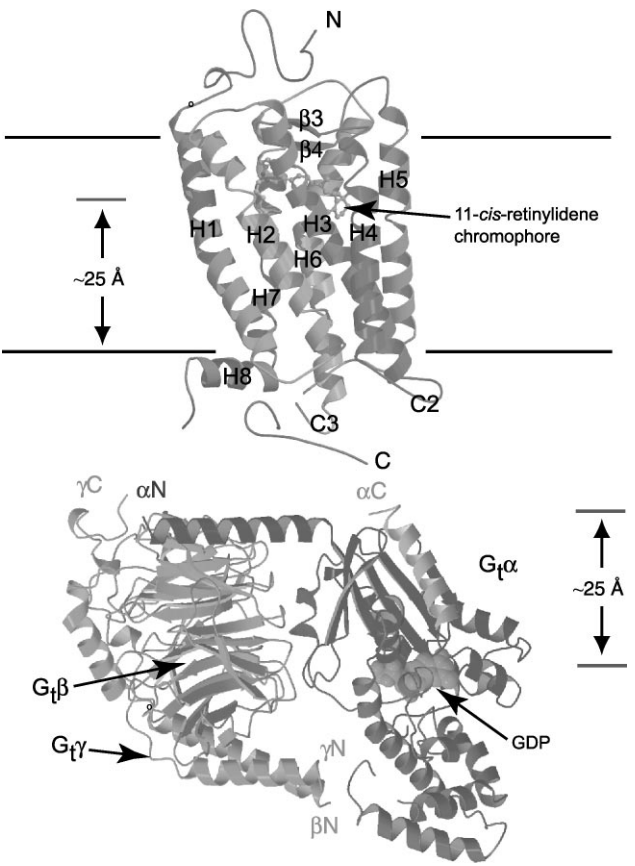

$G\alpha_t$-GTP activates PDE, a tetrameric enzyme consisting of α, β, and γ subunits in a 1:1:2 stoichiometry, by removing the inhibitory constraints that the γ subunits exert upon the catalytic α and β subunits. The binding site of PDE γ on $G\alpha_t$ was recently determined by X-ray crystallography and found to reside between the α2-helix of the Switch II region and the adjacent α3-helix (203).

$G\alpha_t$ hydrolyzes bound GTP to return to its inactive GDP-bound state. Rapid turn-off of the cascade is essential for the temporal resolution of the signal (85). GTP hydrolysis is accelerated by the simultaneous binding of the effector, cGMP PDEγ subunit, and a second protein, regulator of G protein signaling 9 (RGS9) (85). $G\alpha_t$ (GDP) recombines with $G\beta\gamma_t$ and can then be activated again by another R^*.

$G\beta_t$ is a 340–amino acid protein, constructed from an amino-terminal α-helix, followed by a β-propeller structure (204). The β-propeller consists of seven "blades," each consisting of four β-sheets. Each blade is roughly related to the others by rotational symmetry. At the sequence level, $G\beta_t$ is notable for seven WD40 domains, sequence repeats of roughly 40 amino acids that frequently end

←

Figure 4 Interactions between Rho and G_t at the cytoplasmic surface of the disc membrane. A molecular graphics ribbon diagram of Rho prepared from the crystal structure coordinates at 2.8 Å resolution is shown at the *top*. The figure was produced using the A chain of the published crystal structure coordinates (172). The amino terminus (N) and extracellular (or intradiscal) surface is toward the top of the figure and the carboxyl terminus (C) and intracellular (or cytoplasmic) surface is toward the bottom. Seven transmembrane segments (H1 to H7), which are characteristic of GPCRs, are shown. The RET chromophore is shown as a ball and stick model. The Rho crystal structure does not resolve a small segment of the C3 loop linking H5 and H6 or a longer segment of the carboxyl-terminal tail distal to H8. The transmembrane segments are tilted with respect to the presumed plane of the membrane bilayer. They are generally α-helical, but they contain significant kinks and irregularities as described in the text. The chromophore is labeled with an *arrow* pointing to the cyclohexenyl ring. The Schiff base linkage of the chromophore lies approximately 25 Å from the cytoplasmic surface of the membrane bilayer. The structure is the GDP bound form of G_t shown at the bottom with the surface that presumably interacts with Rho facing up. The Ras-like domain of $G\alpha_t$ is above the GDP-binding pocket and the helical domain of $G\alpha_t$ is below. $G\beta_t$ and $G\gamma_t$ are to the left. The bound GDP may be up to 25 Å from the surface of G_t. The amino and carboxyl termini of each subunit are labeled. Structures thought to interact with Rho and/or the membrane, including the amino and carboxyl termini of $G\alpha_t$ and the carboxyl terminus of $G\gamma_t$, cluster on a common surface of G_t. The relative orientation of the cytoplasmic surface of Rho and the Rho-binding surface of G_t is arbitrary. Upon formation of the Rho-G_t complex, the chromophore-binding pocket of Rho becomes allosterically coupled to the nucleotide-binding pocket of G_t, which is approximately 50 Å away. The structure of the R^*-G_t complex has not yet been determined.

with Trp-Asp (WD in the single letter code). Each WD40 repeat corresponds to the fourth strand of one propeller blade and the first three strands of an adjacent blade. $G\beta_t$ is a member of a large family of proteins containing WD40 repeats, which perform a variety of functions; all are thought to fold into β-propeller structures (67, 160). $G\beta_t$ is also a member of a larger family of proteins that fold into β-propeller structures, many of which do not share significant sequence homology.

$G\gamma_t$ is the shortest G_t subunit, consisting of only 73 amino acids. It contains an amino-terminal α-helix, which interacts with the amino terminus of $G\beta_t$ in a coiled-coil conformation (Figure 4). Interestingly, a study conducted prior to the determination of the structure showed that peptides derived from the helical regions of $G\beta_t$ and $G\gamma_t$ do not associate with each other in solution (144). The remainder of $G\gamma_t$ wraps around $G\beta_t$ in an extended conformation. $G\beta_t$ and $G\gamma_t$ can be dissociated from one another only under denaturing conditions, and physiologically they function as a single entity.

The structure of the G_t heterotrimer (122) reveals two distinct sites of interaction between $G\alpha_t$ and $G\beta\gamma_t$: The amino-terminal helix of $G\alpha_t$ interacts with the side of the $G\beta_t$-propeller, and the Switch I/II region of $G\alpha_t$ interacts with the top of the $G\beta_t$-propeller structure. Direct contacts between $G\alpha_t$ and $G\gamma_t$ are not observed in the structure, although interactions between lipids attached to each subunit have been proposed. The structure of free $G\beta\gamma_t$ compared with $G\beta\gamma_t$ in the heterotrimer reveals that $G\beta\gamma_t$ is virtually unchanged by the binding of $G\alpha_t$ (204). However, the structure of $G\alpha_t$ is altered in the conformationally flexible Switch I/II-binding region, which makes contacts with $G\beta_t$ (122). The structure of the amino-terminal helix of $G\alpha_t$ is also likely altered by the binding of $G\beta\gamma_t$.

A number of important posttranslational modifications of G_t have been described. $G\alpha_t$ is heterogeneously acylated, primarily with saturated C_{12} and C_{14} esterified fatty acids, at its amino-terminal glycine (118). This modification is thought to be important for interactions with $G\beta\gamma_t$ (118) and possibly with membranes and rhodopsin (151). Recently, a report describing the phosphorylation of $G\alpha_t$ at Tyr-142 by the tyrosine kinase Src in rod outer segments has been published (20). The significance of this modification is not yet understood. $G\gamma_t$ is modified in a three-step process that includes farnesylation of a cysteine in the carboxyl-terminal CAAX (Cys-Ala-Ala-X) motif, cleavage of the three carboxyl-terminal amino acids, and carboxymethylation of the free carboxyl terminus (226). Farnesylation has been found to be important for interactions with $G\alpha_t$ (145) as well as with rhodopsin (109, 198). There is evidence that rhodopsin can discriminate between farnesyl (C_{15}) and geranylgeranyl (C_{20}) esterified fatty acids (109), which suggests the existence of a specific prenyl-binding site on Rho.

Many biochemical and biophysical techniques have been used to identify sites on G_t that interact with membranes and with R^*. The involvement of the carboxyl-terminal 11 amino acids of $G\alpha_t$ (a.a. 340–350) in interactions with R^* is suggested by many studies, including (*a*) the finding that Pertussis toxin catalyzes the ADP-ribosylation of Cys-347, which uncouples G_t from R^*; (*b*) a peptide corresponding to amino acids 340–350 can uncouple R^* from G_t and can itself bind to R^* and

mimic the effects of G_t (78, 111); (*c*) site-directed mutagenesis (66, 170); and (*d*) the demonstration in related G proteins that specificity of coupling to particular receptors resides in their carboxyl termini (37). In addition, peptide competition and site-directed mutagenesis studies have suggested the involvement of the $\alpha 4/\beta 6$ loop of $G\alpha_t$, which lies adjacent to the carboxyl terminus, in interacting with R^* (78, 159). Experimental evidence suggests that $G\beta\gamma_t$ is also in direct contact with rhodopsin (105, 178). The specific contacts between $G\beta\gamma_t$ and R^* involve the carboxyl terminus of $G\gamma_t$, as suggested by studies with peptides derived from that region (108, 109) and possibly the seventh propeller blade of $G\beta\gamma_t$ (217).

All the structures of G_t that are thought to participate in interactions with Rho or the membrane cluster to a common face on the structure of G_t and identify a putative Rho-interacting surface (25, 122) (Figure 4). However, in the crystal structure of the heterotrimer, neither the carboxyl terminus of $G\alpha_t$ nor that of $G\gamma_t$ are included. Thus, the structure of the specific Rho-interacting regions is unclear. A partial remedy has been provided by an NMR study of a peptide derived from the carboxyl terminus of $G\alpha_t$ in its Rho-bound conformation; these data suggest that it forms an extension of the $\alpha 5$-helix of $G\alpha_t$ (110).

The Mechanism of Rhodopsin-Catalyzed Nucleotide Exchange

The photoisomerization of 11-*cis*-retinal to ATR leads to local structural alterations in the chromophore-binding pocket of Rho. These structural changes are propagated to the cytoplasmic surface of Rho, and following binding of G_t, on to the nucleotide-binding pocket of $G\alpha_t$ where GDP is released. In this way, the chromophore-binding pocket of Rho is allosterically coupled to the nucleotide-binding pocket of $G\alpha_t$ approximately 5 nm away (Figure 4). Several key observations characterize the process of R^*-catalyzed nucleotide exchange. In the absence of a catalyst, the rate-limiting step in nucleotide exchange is release of GDP from $G\alpha_t$ to form empty-pocket G_t, $G\alpha_t(e)\beta\gamma_t$. $G\alpha_t(e)$ is by itself very unstable. R^* catalyzes nucleotide exchange by inducing GDP release and stabilizing the reaction intermediate, $G\alpha_t(e)\beta\gamma_t$. The empty-pocket G_t can be dissociated from R^* by either GDP or GTP; R^* and nucleotide binding are mutually exclusive. GTP binding is nearly irreversible since conformational changes in the Switch II region destroy the $G\beta\gamma_t$-binding site and induce dissociation of $G\alpha_t$(GTP) from $G\beta\gamma_t$ and R^*. R^* interacts specifically with heterotrimeric G_t; $G\beta\gamma_t$ appears to be absolutely required for efficient R^*-catalyzed nucleotide exchange on $G\alpha_t$ (61). It is unclear whether $G\beta\gamma_t$ plays a mechanistic role in catalysis (95) or whether it merely facilitates binding between Rho and $G\alpha_t$ (179). Binding of G_t to R^* and dissociation of GDP appear to be distinct steps; Rho mutants that bind G_t but do not induce GDP release have been described (45, 59).

The molecular mechanism by which R^* induces GDP release from G_t is the least-understood step in the G_t signaling cycle. Despite a great deal of data regarding structures of G_t and Rho that interact with each other, little is known about the detailed structure of the complex (133). The structure of R^* is not known, and

the conformational changes, if any, that occur in R^* and G_t-GDP upon complex formation are not known. Few sites of point-to-point contacts between R^* and G protein have been reliably identified (4), and those that have been found do not greatly constrain possible geometric alignments of the two proteins in the complex. Crystallographic analysis of the R^*-G_t(e) complex may prove difficult owing to the instability of R^*. The alignment of the interacting surfaces in the structures of Rho and G_t produces a hypothetical low-resolution model of the complex (28) (Figure 4). These analyses, although lacking details, do suggest clearly that the cytoplasmic loops of Rho, which are roughly 1.5 nm long (at most) are too short to contact directly the nucleotide-binding pocket of $G\alpha_t$, which is at least 2.5 nm from the Rho-binding surface of G_t. Consequently, R^* must act "at-a-distance" to induce nucleotide exchange in $G\alpha_t$ (95).

One long-standing hypothesis regarding the mechanism of nucleotide exchange suggested that interdomain interactions between amino acid side chains of the Ras-like and the helical domains of $G\alpha_t$ regulated nucleotide exchange rate. Recently, Marin et al. developed a method to assay the rates of both uncatalyzed and R^*-catalyzed nucleotide exchange of $G\alpha_t$ and $G\alpha_t$ mutants expressed in vitro (141). They demonstrated that contrary to what was predicted, disruption of interdomain interactions by site-directed mutations did not affect either basal or R^*-catalyzed nucleotide exchange rates in $G\alpha_t$ (141). However, additional studies identified a cluster of residues on the α5-helix, which, when mutated, dramatically accelerated nucleotide exchange. These results suggested a key role for the α5-helix of $G\alpha_t$ in mediating nucleotide exchange. The α5-helix connects the carboxyl terminus to the β6/α5 loop, which lies adjacent to the nucleotide. It is possible that the binding of R^* to this region of $G\alpha_t$ perturbs key stabilizing interactions to induce GDP release (142).

Additional Protein-Protein Interactions

A number of cytoplasmic proteins besides G_t are known to interact with R^*. These include Rho kinase, which phosphorylates R^* at specific serine residues (Ser-334, Ser-338, and Ser-343) (147, 165, 174). Reconstitution experiments suggest that light-dependent phosphorylation of Rho is catalyzed primarily by Rho kinase and not by protein kinase C (166). Phosphorylation decreases the effective lifetime of R^* but paradoxically shifts the M-I/M-II equilibrium toward M-II (70). Signal quenching requires that arrestin binds to phosphorylated R^* to prevent it from activating G_t. The role of the distal carboxyl-terminal tail in the shut-off of the light signal in the rod cell was shown convincingly in a study using a transgenic mouse strain. The mice, whose rod cells expressed a Rho transgene with a truncated carboxyl-terminal tail, were studied by electrophysiological techniques. Phosphorylation of the carboxyl-terminal tail was required for termination of light-induced signaling (35). The current state of the structural biology of proteins involved in vertebrate phototransduction is summarized in Table 1 (available as Supplemental Material: follow the Supplemental Material link on the Annual Reviews homepage at http://www.annualreviews.org/).

STRUCTURAL STUDIES OF BACTERIORHODOPSIN

Although Rho shares no primary structural homology with archaebacterial retinal-based ion pumps or sensory pigments, some obvious similarities do exist. The general molecular topology is conserved among visual pigments and archaebacterial retinal-based pigments because of the existence in both classes of seven TM segments and an extracellular N-terminal tail. In addition, the retinylidene chromophore in all cases is bound to a lysine residue on H-7 through a Schiff base linkage. A detailed discussion of archaebacterial pigments is beyond the intended scope of this chapter. However, since several high-resolution structures have recently become available, particularly of bacteriorhodopsin (bR), the light-driven proton pump of *Halobacterium salinarium*, a short summary is presented below. A comparison of the crystal structures of Rho and bR has also been recently discussed (218).

Recent advances in the refinement of X-ray crystallographic structural detail in bR have helped to elucidate its proton-pumping mechanism, particularly with respect to the involvement of internal water molecules in the vectorial transfer of protons through the translocation channel. A major breakthrough in the structural biology of bR was achieved a decade ago by high-resolution electron cryomicroscopy at 3.5 Å resolution (88). There followed a number of refinements, notably correcting electron-crystallographic data for diffuse scattering and the addition of phase information (73). Attempts to obtain crystals of bR suitable for X-ray diffraction measurements were not successful for a number of years presumably because removal from the phospholipid membrane, even by mild detergent, caused structural inhomogeneities. The development of lipidic cubic phases for the crystallization of membrane proteins made possible the preparation of three-dimensional hexagonal plate-like crystals of bR and of mutants of bR (123, 177). The bicontinuous lipidic cubic phase is an ordered three-dimensional matrix perforated by a regular channel system that allows free diffusion of hydrophilic as well as hydrophobic solutes. The size of the hexagonal plate-like bR crystals was typically in the range of $80 \times 80 \times 15$ μm (21, 138). The use of high-energy X-rays made possible short exposure times at low temperatures (microfocus beamline from a synchrotron, λ close to 1.000 Å, 120 frames at 30 sec/frame, 110 K). These conditions cause a minimum of damage to the reactive molecule and may also be used to determine structures of reaction intermediates in the photocycle. bR structures with resolutions of 1.9 Å (21) and 1.55 Å (140) have been reported.

Minimal conformational changes are apparent in the TM helices during the initial fast kinetics steps of the bR photocycle, when the intermediates K (590 nm) and L (550 nm) are observed (138). The L $\rightarrow$ M step involves the deprotonation of the positively charged Schiff base at Lys-216. It is well established that the Schiff base is deprotonated only in the M intermediate during the photocycle. There is strong evidence that there are two variants, M1 (412 nm) and M2 (412 nm), also designated as early M and late M. The two species are distinguished kinetically (23) and can be detected in FTIR double-flash experiments (90). Discussion continues

regarding the details of structural and conformational changes during the M formation and decay (103). A reasonable sequence of occurrences is that L → M1 → M2 constitutes first the deprotonation of the Schiff base by transfer of a proton to the carboxylate of Asp-85 with outward bending of H-3, facilitating exposure to the extracellular surface, followed by the release of a proton from Glu-204 to an extracellular water molecule.

The reaction M (412 nm) → N (560 nm) restores the protonation of the Schiff base by transfer of a proton from Asp-96 (138). With the formation of intermediate N, H-3 has regained its original conformation and the cytoplasmic half of the H-6 is bent outward, allowing the H-7 to approach Lys-216 to provide closer proximity of Asp-96 to the Schiff base. The chromophore is still in its 13-*cis*, 15-*anti* configuration. Protonation of Asp-96 occurs in the reaction step N (560 nm) → O (610 nm). The proton is supplied by a cytoplasmic water molecule. In the final step O (610 nm) → bR (568 nm), the chromophore undergoes isomerization to all-*trans*, and the TM helices return to their original conformation as in light-adapted bR at the start of the photocycle.

The identity of the photocycle intermediates is well established kinetically. The ground-state bR (568 nm), M (412 nm), N (560 nm), and O (610 nm) are distinguished spectroscopically in the UV-visible range associated with $\pi \rightarrow \pi^*$ transitions of the conjugated double-bond system of the chromophore. Free retinal has a maximal absorption at approximately 380 nm, and the shifts are clearly a result of interactions with the opsin moiety. The photocycle intermediates are well resolved kinetically because their formation and decay occur during very different time frames (six orders of magnitude, ns to ms). Conformational changes in the TM helices and in the movement of water molecules H-bonded to amino acid side chains can be observed spectroscopically in the infrared region (101) and also by ^{13}C-NMR (191) and ^{15}N-NMR (89).

An early model for proton transduction by bR, proposed more than a decade ago, was known as the proton-wire model, where the wire was located in the "proton pathway channel" between the TM helices. This concept was based on the Grotthuss mechanism for the transport of hydrogen ions in liquid water (151a). The proton-wire hypothesis was short-lived because it became evident that amino acid side chains, such as carboxylate and carboxyl, were directly involved in proton pumping and that the deprotonation and reprotonation of the Schiff base were central to the proton translocation process. For a number of years there remained the difficulty that X-ray crystallographic structures showed distances to be too large between the Schiff base and the candidate acceptor amino acid residues, such as Asp-85 and Asp-96, for a direct transfer of a proton to take place. The postulate that water molecules located in the proton pathway channel could bridge the gap was not difficult to accept, even though such molecules eluded direct observation. In recent years FTIR, NMR, and high-resolution crystallographic methods have provided direct evidence for specific water molecules forming a H-bonded network associated with specific prototropic amino acid side chain groups (41, 64, 100, 138, 140, 152, 177). The amino acid residues are located at

specific points in the amino acid sequence, and the participating side chains are therefore tethered to the peptide backbone of the TM helices, although some freedom of movement is still possible (72). By contrast, the participating water molecules are localized within a cage but are ultimately exchangeable with water molecules in the cytoplasm and in the extracellular medium.

The currently emerging details of the proton translocation mechanism in bR point to simultaneous concerted movements in the conformation of segments of the TM helices, orientation of amino acid side chains, acceptance and release of protons by prototropic groups, redistribution of electrostatic charges, and configuration and orientation of the chromophore. The effects of electrostatic charges at critical points provide vectoriality in the proton translocation by electrostatic steering (89, 197). Time-resolved crystallographic structure determination, termed kinetic crystallography, could ultimately establish the complete mechanism of light-driven proton pumping (2, 94, 139, 162, 177). It is hoped that future high-resolution structures of Rho, Rho photoproducts, and mutants of Rho will allow the function of Rho to be elucidated with a similar degree of detail.

CONCLUSION

Rho is a paradox. On the one hand, it displays several unique and fascinating properties that allow it to function as the dim-light photoreceptor in the rod cell. It has an extremely low rate of thermal activation, but it can be activated by a single photon at high quantum efficiency. On the other hand, it serves as a prototype of the largest family of membrane receptors in the human genome, GPCRs. The recent report of the crystal structure of bovine Rho provides a unique opportunity to address questions related to the structural basis of Rho function in the vertebrate visual transduction cascade. Over the past decade a remarkable amount of information about structure-activity relationships in Rho, and other GPCRs, has been obtained using techniques of molecular biology. The crystal structure of Rho also provides a chance to evaluate the quality of this information. Site-directed mutant pigments have been employed to elucidate key structural elements, the opsin-shift mechanism and the mechanism of receptor photoactivation.

Perhaps the greatest surprise in the crystal structure was the role of the extracellular surface domain in defining the RET-binding pocket. Whether this feature carries over to other GPCRs remains to be determined. One particular advantage of studying Rho has been the opportunity to employ various spectroscopic methods, especially in combination with site-directed mutagenesis. Optical spectroscopy and resonance Raman spectroscopy are possible because of the presence of the RET chromophore, which is probed as a sensor of chromophore-protein interactions. Difference spectroscopy techniques, such as FTIR- and UV-visible-difference spectroscopy, make use of the chromophore as an optical switch. Overexpression of recombinant Rho allows a variety of biophysical methods to be used to address particular questions related to protein and chromophore conformational changes. Important future work will involve questions related to the precise molecular

mechanism of signal transduction by Rho. This will require some understanding of the dynamic changes in protein conformation, not only in Rho, but in the other proteins of the vertebrate visual cascade.

ACKNOWLEDGMENTS

We gratefully acknowledge the members of the Laboratory of Molecular Biology and Biochemistry at The Rockefeller University, including students, postdoctoral fellows, and associates, who have worked on visual phototransduction over the past ten years. In addition, productive collaborations with several exceptional laboratories have been greatly appreciated. Support was provided by NIH Training Grants (GM 07739 and EY 07138), the Charles H. Revson Foundation, the Aaron Diamond Foundation, the Arts and Letters Foundation, and the Allene Reuss Memorial Trust. T. P. Sakmar is an associate investigator of the Howard Hughes Medical Institute and an Ellison Foundation Senior Scholar.

LITERATURE CITED

1. Abdulaev NG, Ridge KD. 1998. Light-induced exposure of the cytoplasmic end of transmembrane helix seven in rhodopsin. *Proc. Natl. Acad. Sci. USA* 95:12854–59
2. Abola E, Kuhn P, Earnest T, Stevens RC. 2000. Automation of X-ray crystallography. *Nat. Struct. Biol.* 7:973–77
3. Acharya S, Karnik SS. 1996. Modulation of GDP release from transducin by the conserved Glu134-Arg135 sequence in rhodopsin. *J. Biol. Chem.* 271:25406–11
4. Acharya S, Saad Y, Karnik SS. 1997. Transducin-alpha C-terminal peptide binding site consists of C–D and E–F loops of rhodopsin. *J. Biol. Chem.* 272: 6519–24
5. Alkorta I, Du P. 1994. Sequence divergence analysis for the prediction of seven-helix membrane protein structures. II. A 3-D model of human rhodopsin. *Protein Eng.* 7:1231–38
6. Altenbach C, Cai K, Khorana HG, Hubbell WL. 1999. Structural features and light-dependent changes in the sequence 306–322 extending from helix VII to the palmitoylation sites in rhodopsin: a site-directed spin-labeling study. *Biochemistry* 38:7931–37
7. Altenbach C, Klein -Seetharaman J, Hwa J, Khorana HG, Hubbell WL. 1999. Structural features and light-dependent changes in the sequence 59–75 connecting helices I and II in rhodopsin: a site-directed spin-labeling study. *Biochemistry* 38:7945–49
8. Ames JB, Dizhoor AM, Ikura M, Palczewski K, Stryer L. 1999. Three-dimensional structure of guanylyl cyclase activating protein-2, a calcium-sensitive modulator of photoreceptor guanylyl cyclases. *J. Biol. Chem.* 274:19329–37
9. Anukanth A, Khorana HG. 1994. Structure and function in rhodopsin. Requirements of a specific structure for the intradiscal domain. *J. Biol. Chem.* 269: 19738–44
10. Arnis S, Fahmy K, Hofmann KP, Sakmar TP. 1994. A conserved carboxylic acid group mediates light-dependent proton

uptake and signaling by rhodopsin. *J. Biol. Chem.* 269:23879–81
11. Asenjo AB, Rim J, Oprian DD. 1994. Molecular determinants of human red/green color discrimination. *Neuron* 12: 1131–38
12. Baldwin JM, Schertler GF, Unger VM. 1997. An alpha-carbon template for the transmembrane helices in the rhodopsin family of G-protein-coupled receptors. *J. Mol. Biol.* 272:144–64
13. Ballesteros JA, Shi L, Javitch JA. 2001. Structural mimicry in G protein-coupled receptors: implications of the high-resolution structure of rhodopsin for structure-function analysis of rhodopsin-like receptors. *Mol. Pharmacol.* 60:1–19
14. Baylor DA. 1987. Photoreceptor signals and vision. Proctor lecture. *Invest. Ophthalmol. Vis. Sci.* 28:34–49
15. Baylor DA. 1996. How photons start vision. *Proc. Natl. Acad. Sci. USA* 93:560–65
16. Baylor DA, Lamb TD, Yau KW. 1979. Responses of retinal rods to single photons. *J. Physiol.* 288:613–34
17. Baylor DA, Lamb TD, Yau KW. 1979. The membrane current of single rod outer segments. *J. Physiol.* 288:589–611
18. Beck M, Sakmar TP, Siebert F. 1998. Spectroscopic evidence for interaction between transmembrane helices 3 and 5 in rhodopsin. *Biochemistry* 37:7630–39
19. Beck M, Siebert F, Sakmar TP. 1998. Evidence for the specific interaction of a lipid molecule with rhodopsin which is altered in the transition to the active state metarhodopsin II. *FEBS Lett.* 436:304–8
20. Bell MW, Desai N, Guo XX, Ghalayini AJ. 2000. Tyrosine phosphorylation of the alpha subunit of transducin and its association with Src in photoreceptor rod outer segments *J. Neurochem.* 75:2006–19
21. Belrhali H, Nollert P, Royant A, Menzel C, Rosenbusch JP, et al. 1999. Protein, lipid and water organization in bacteriorhodopsin crystals: a molecular view of the purple membrane at 1.9 Å resolution. *Struct. Fold Des.* 7:909–17
22. Benovic JL, Mayor F Jr, Somers RL, Caron MG, Lefkowitz RJ. 1986. Light-dependent phosphorylation of rhodopsin by beta-adrenergic receptor kinase. *Nature* 321:869–72
23. Betancourt FM, Glaeser RM. 2000. Chemical and physical evidence for multiple functional steps comprising the M state of the bacteriorhodopsin photocycle. *Biochim. Biophys. Acta* 1460:106–18
24. Birge RR, Murray LP, Pierce BM, Akita H, Balogh-Nair V, et al. 1985. Two-photon spectroscopy of locked-11-*cis*-rhodopsin: evidence for a protonated Schiff base in a neutral protein binding site. *Proc. Natl. Acad. Sci. USA* 82:4117–21
25. Bohm A, Gaudet R, Sigler PB. 1997. Structural aspects of heterotrimeric G-protein signaling. *Curr. Opin. Biotechnol.* 8:480–87
26. Borhan BM, Souto L, Imai H, Shichida Y, Nakanishi K. 2000. Movement of retinal along the visual transduction path. *Science* 288:2209–12
27. Borjigin J, Nathans J. 1994. Insertional mutagenesis as a probe of rhodopsin's topography, stability, and activity. *J. Biol. Chem.* 269:14715–22
28. Bourne HR. How receptors talk to trimeric G proteins. 1997. *Curr. Opin. Cell. Biol.* 9:134–42
29. Buczylko J, Saari JC, Crouch RK, Palczewski K. 1996. Mechanisms of opsin activation. *J. Biol. Chem.* 271:20621–30
30. Cai K, Klein-Seetharaman J, Farrens D, Zhang C, Altenbach C, et al. 1999. Single-cysteine substitution mutants at amino acid positions 306–321 in rhodopsin, the sequence between the cytoplasmic end of helix VII and the palmitoylation sites: Sulfhydryl reactivity and transducin activation reveal a tertiary structure. *Biochemistry* 38:7925–30

31. Cha K, Reeves PJ, Khorana HG. 2000. Structure and function in rhodopsin: Destabilization of rhodopsin by the binding of an antibody at the N-terminal segment provides support for involvement of the latter in an intradiscal tertiary structure. *Proc. Natl. Acad. Sci. USA* 97: 3016–21
32. Chabre M. 1985. Trigger and amplification mechanisms in visual phototransduction. *Annu. Rev. Biophys. Biophys. Chem.* 14:331–60
33. Chabre M, Breton J. 1979. Orientation of aromatic residues in rhodopsin. Rotation of one tryptophan upon the meta I to meta II transition after illumination. *Photochem. Photobiol.* 30:295–99
34. Chan T, Lee M, Sakmar TP. 1992. Introduction of hydroxyl-bearing amino acids causes bathochromic spectral shifts in rhodopsin. Amino acid substitutions responsible for red-green color pigment spectral tuning. *J. Biol. Chem.* 267: 9478–80
35. Chen J, Makino CL, Peachey NS, Baylor DA, Simon MI. 1995. Mechanisms of rhodopsin inactivation in vivo as revealed by a COOH-terminal truncation mutant. *Science* 267:374–77
36. Cohen GB, Oprian DD, Robinson PR. 1992. Mechanism of activation and inactivation of opsin: role of Glu113 and Lys296. *Biochemistry* 31:12592–601
37. Conklin BR, Farfel Z, Lustig KD, Julius D, Bourne HR. 1993. Substitution of three amino acids switches receptor specificity of Gq alpha to that of Gi alpha. *Nature* 363:274–76
38. Creemers AF, Klaassen CH, Bovee-Geurts PH, Kelle R, Kragl U, et al. 1999. Solid state ^{15}N NMR evidence for a complex Schiff base counterion in the visual G-protein-coupled receptor rhodopsin. *Biochemistry* 38:7195–99
39. Davidson FF, Loewen PC, Khorana HG. 1994. Structure and function in rhodopsin: Replacement by alanine of cysteine residues 110 and 187, components of a conserved disulfide bond in rhodopsin, affects the light-activated metarhodopsin II state. *Proc. Natl. Acad. Sci. USA* 91: 4029–33
40. DeLange F, Bovee-Geurts PH, Pistorius AM, Rothschild KJ, DeGrip WJ. 1999. Probing intramolecular orientations in rhodopsin and metarhodopsin II by polarized infrared difference spectroscopy. *Biochemistry* 38:13200–9
41. Dencher NA, Sass HJ, Büldt G. 2000. Water and bacteriorhodopsin: structure, dynamics, and function. *Biochim. Biophys. Acta* 1460:192–203
42. Doi T, Molday RS, Khorana HG. 1990. Role of the intradiscal domain in rhodopsin assembly and function. *Proc. Natl. Acad. Sci. USA* 87:4991–95
43. Dunham TD, Farrens DL. 1999. Conformational changes in rhodopsin. Movement of helix f detected by site-specific chemical labeling and fluorescence spectroscopy. *J. Biol. Chem.* 274:1683–90
44. Eilers M, Reeves PJ, Ying W, Khorana HG, Smith SO. 1999. Magic angle spinning NMR of the protonated retinylidene Schiff base nitrogen in rhodopsin: expression of ^{15}N-lysine- and ^{13}C-glycine-labeled opsin in a stable cell line. *Proc. Natl. Acad. Sci. USA* 96:487–92
45. Ernst OP, Hofmann KP, Sakmar TP. 1995. Characterization of rhodopsin mutants that bind transducin but fail to induce GTP nucleotide uptake. Classification of mutant pigments by fluorescence, nucleotide release, and flash-induced light-scattering assays. *J. Biol. Chem.* 270:10580–86
46. Ernst OP, Meyer CK, Marin EP, Henklein P, Fu WY, et al. 2000. Mutation of the fourth cytoplasmic loop of rhodopsin affects binding of transducin and peptides derived from the carboxyl-terminal sequences of transducin alpha and gamma subunits. *J. Biol. Chem.* 275:1937–43
47. Fahmy K. 1998. Binding of transducin and transducin-derived peptides to

rhodopsin studies by attenuated total reflection-Fourier transform infrared difference spectroscopy. *Biophys. J.* 75: 1306–18
48. Fahmy K, Jäger F, Beck M, Zvyaga TA, Sakmar TP, Siebert F. 1993. Protonation states of membrane-embedded carboxylic acid groups in rhodopsin and metarhodopsin II: a Fourier-transform infrared spectroscopy study of site-directed mutants. *Proc. Natl. Acad. Sci. USA* 90:10206–10
49. Fahmy K, Sakmar TP. 1993. Light-dependent transducin activation by an ultraviolet-absorbing rhodopsin mutant. *Biochemistry* 32:9165–71
50. Fahmy K, Sakmar TP. 1993. Regulation of the rhodopsin-transducin interaction by a highly conserved carboxylic acid group. *Biochemistry* 32:7229–36
51. Fahmy K, Sakmar TP, Siebert F. 2000. Structural determinants of active state conformation of rhodopsin: molecular biophysics approaches. *Methods Enzymol.* 315:178–96
52. Fahmy K, Sakmar TP, Siebert F. 2000. Transducin-dependent protonation of glutamic acid 134 in rhodopsin. *Biochemistry* 39:10607–12
53. Fahmy K, Siebert F, Sakmar TP. 1995. Photoactivated state of rhodopsin and how it can form. *Biophys. Chem.* 56:171–81
54. Farahbakhsh ZT, Hideg K, Hubbell WL. 1993. Photoactivated conformational changes in rhodopsin: a time-resolved spin label study. *Science* 262:1416–19
55. Farrens DL, Altenbach C, Yang K, Hubbell WL, Khorana HG. 1996. Requirement of rigid-body motion of transmembrane helices for light activation of rhodopsin. *Science* 274:768–70
56. Faurobert E, Otto-Bruc A, Chardin P, Chabre M. 1993. Tryptophan W207 in transducin Talpha is the fluorescence sensor of the G protein activation switch and is involved in the effector binding. *EMBO J.* 12:4191–98
57. Feng X, Verdegem PJ, Eden M, Sandstrom D, Lee YK, et al. 2000. Determination of a molecular torsional angle in the metarhodopsin-I photointermediate of rhodopsin by double-quantum solid-state NMR. *J. Biomol. Nucl. Magn. Res.* 16:1–8
58. Flaherty KM, Zozulya S, Stryer L, McKay DB. 1993. Three-dimensional structure of recoverin, a calcium sensor in vision. *Cell* 75:709–16
59. Franke RR, Konig B, Sakmar TP, Khorana HG, Hofmann KP. 1990. Rhodopsin mutants that bind but fail to activate transducin. *Science* 250:123–25
60. Franke RR, Sakmar TP, Graham RM, Khorana HG. 1992. Structure and function in rhodopsin. Studies of the interaction between the rhodopsin cytoplasmic domain and transducin. *J. Biol. Chem.* 267:14767–74
61. Fung BKK. 1983. Characterization of transducin from bovine retinal rod outer segments. I. Separation and reconstitution of the subunits. *J. Biol. Chem.* 258: 10495–502
62. Fung BKK, Nash CR. 1983. Characterization of transducin from bovine retinal rod outer segments. II. Evidence for distinct binding sites and conformational changes revealed by limited proteolysis with trypsin. *J. Biol. Chem.* 258:10503–10
63. Fung BKK, Stryer L. 1980. Photolyzed rhodopsin catalyzes the exchange of GTP for bound GDP in retinal rod outer segments. *Proc. Natl. Acad. Sci. USA* 77:2500–4
64. Ganea C, Gergely C, Ludmann K, Varo G. 1997. The role of water in the extracellular half channel of bacteriorhodopsin. *Biophys. J.* 73:2718–25
65. Ganter UM, Kashima T, Sheves M, Siebert F. 1991. FTIR evidence of an altered chromophore-protein-interaction in the artificial visual pigment *cis*-5,6-dihydroisorhodopsin and its photoproducts BSI,

lumirhodopsin and metarhodopsin-I. *J. Am. Chem. Soc.* 113:4087–92
66. Garcia PD, Onrust R, Bell SM, Sakmar TP, Bourne HR. 1995. Transducin-alpha C-terminal mutations prevent activation by rhodopsin: a new assay using recombinant proteins expressed in cultured cells. *EMBO J.* 14:4460–69
67. Garcia-Higuera I, Fenoglio J, Li Y, Lewis C, Panchenko MP, et al. 1996. Folding of proteins with WD-repeats: comparison of six members of the WD-repeat superfamily to the G protein beta subunit. *Biochemistry* 35:13985–94
68. Gaudet R, Bohm A, Sigler PB. 1996. Crystal structure at 2.4 Å resolution of the complex of transducin beta-gamma and its regulator, phosducin. *Cell* 87:577–88
69. Gether U. 2000. Uncovering molecular mechanisms involved in activation of G protein-coupled receptors. *Endocr. Rev.* 21:90–113
70. Gibson SK, Parkes JH, Liebman PA. 1999. Phosphorylation alters the pH-dependent active state equilibrium of rhodopsin by modulating the membrane surface potential. *Biochemistry* 38: 11103–14
71. Granzin J, Wilden U, Choe HW, Labahn J, Krafft B, Büldt G. 1998. X-ray crystal structure of arrestin from bovine rod outer segments. *Nature* 391:918–21
72. Griffiths JM, Bennett AE, Engelhard M, Siebert F, Raap J, et al. 2000. Structural investigation of the active site in bacteriorhodopsin: geometric constraints on the roles of Asp-85 and Asp-212 in the proton-pumping mechanism from solid state NMR. *Biochemistry* 39:362–71
73. Grigorieff N, Ceska TA, Downing KH, Baldwin JM, Henderson R. 1996. Electron-crystallographic refinement of the structure of bacteriorhodopsin. *J. Mol. Biol.* 259:393–421
74. Grobner G, Burnett IJ, Glaubitz C, Choi G, Mason AJ, Watts A. 2000. Observations of light-induced structural changes of retinal within rhodopsin. *Nature* 405: 810–13
75. Grobner G, Choi G, Burnett IJ, Glaubitz C, Verdegem PJ, et al. 1998. Photoreceptor rhodopsin: structural and conformational study of its chromophore 11-*cis* retinal in oriented membranes by deuterium solid state NMR. *FEBS Lett.* 422: 201–4
76. Deleted in proof
77. Groves MR, Hanlon N, Turowski P, Hemmings BA, Barford D. 1999. The structure of the protein phosphatase 2A PR65/A subunit reveals the conformation of its 15 tandemly repeated HEAT motifs. *Cell* 96:99–110
78. Hamm HE, Deretic D, Arendt A, Hargrave PA, Koenig B, Hofmann KP. 1988. Site of G protein binding to rhodopsin mapped with synthetic peptides from the α subunit. *Science* 241:832–35
79. Han M, Lin SW, Minkova M, Smith SO, Sakmar TP. 1996. Functional interaction of transmembrane helices 3 and 6 in rhodopsin. Replacement of phenylalanine 261 by alanine causes reversion of phenotype of a glycine 121 replacement mutant. *J. Biol. Chem.* 271:32337–42
80. Han M, Lin SW, Smith SO, Sakmar TP. 1996. The effects of amino acid replacements of glycine 121 on transmembrane helix 3 of rhodopsin. *J. Biol. Chem.* 271:32330–36
81. Han M, Smith SO. 1995. NMR constraints on the location of the retinal chromophore in rhodopsin and bathorhodopsin. *Biochemistry* 34:1425–32
82. Han M, Smith SO, Sakmar TP. 1998. Constitutive activation of opsin by mutation of methionine 257 on transmembrane helix 6. *Biochemistry* 37:8253–61
83. Hargrave PA, Bownds D, Wang JK, McDowell JH. 1982. Retinyl peptide isolation and characterization. *Methods Enzymol.* 81:211–14
84. Hargrave PA, McDowell JH, Curtis DR, Wang JK, Juszczak E, et al. 1983. The

structure of bovine rhodopsin. *Biophys. Struct. Mech.* 9:235–44
85. He W, Cowan CW, Wensel TG. 1998. RGS9, a GTPase accelerator for phototransduction. *Neuron* 20:95–102
86. Hecht S, Shaler S, Pirene MH. 1942. Energy, quanta, and vision. *J. Gen. Physiol.* 25:819–40
87. Heck M, Hofmann KP. 2001. Maximal rate and nucleotide dependence of rhodopsin-catalyzed transducin activation: initial rate analysis based on a double displacement mechanism. *J. Biol. Chem.* 276:10000–9
88. Henderson R, Baldwin JM, Ceska TA, Zemlin F, Beckmann E, Downing KH. 1990. An atomic model for the structure of bacteriorhodopsin. *Biochem. Soc. Trans.* 18:844
89. Herzfeld J, Tounge B. 2000. NMR probes of vectoriality in the proton-motive photocycle of bacteriorhodopsin: evidence for an "electrostatic steering" mechanism. *Biochim. Biophys. Acta* 1460:95–105
90. Hessling B, Herbst J, Rammelsberg R, Gerwert K. 1997. Fourier transform infrared double-flash experiments resolve bacteriorhodopsin's M1 to M2 transition. *Biophys. J.* 73:2071–80
91. Hirsch JA, Schubert C, Gurevich VV, Sigler PB. 1999. The 2.8 Å crystal structure of visual arrestin: a model for arrestin's regulation. *Cell* 97:257–69
92. Honig B, Dinur U, Nakanishi K, Balogh-Nair V, Gawinowicz MA, et al. 1979. An external point-charge model for wavelength regulation in visual pigments. *J. Am. Chem. Soc.* 101:7084–86
93. Huang L, Deng H, Koutalos Y, Ebrey T, Groesbeek M, et al. 1997. A resonance Raman study of the C=C stretch modes in bovine and octopus visual pigments with isotopically labeled retinal chromophores. *Photochem. Photobiol.* 66: 747–54
94. Hwa J, Reeves PJ, Klein-Seetharaman J, Davidson F, Khorana HG. 1999. Structure and function in rhodopsin: further elucidation of the role of the intradiscal cysteines, Cys-110, -185, and -187, in rhodopsin folding and function. *Proc. Natl. Acad. Sci. USA* 96:1932–35
95. Iiri T, Farfel Z, Bourne HR. 1998. G-protein diseases furnish a model for the turn-on switch. *Nature* 394:35–38
96. Isele J, Sakmar TP, Siebert F. 2000. Rhodopsin activation affects the environment of specific neighboring phospholipids: an FTIR study. *Biophys. J.* 79:3063–71
97. Jäger F, Fahmy K, Sakmar TP, Siebert F. 1994. Identification of glutamic acid 113 as the Schiff base proton acceptor in the metarhodopsin II photointermediate of rhodopsin. *Biochemistry* 33:10878–82
98. Jäger F, Jäger S, Krutle O, Friedman N, Sheves M, et al. 1994. Interactions of the beta-ionone ring with the protein in the visual pigment rhodopsin control the activation mechanism. An FTIR and fluorescence study on artificial vertebrate rhodopsins. *Biochemistry* 33:7389–97
99. Jäger S, Szundi I, Lewis JW, Mah TL, Kliger DS. 1998. Effects of pH on rhodopsin photointermediates from lumirhodopsin to metarhodopsin II. *Biochemistry* 37:6998–7005
100. Kandori H. 2000. Role of internal water molecules in bacteriorhodopsin. *Biochim. Biophys. Acta* 1460:177–91
101. Kandori H, Kinoshita N, Yamazaki Y, Maeda A, Shichida Y, et al. 2000. Local and distant protein structural changes on photoisomerization of the retinal in bacteriorhodopsin. *Proc. Natl. Acad. Sci. USA* 97:4643–48
102. Karnik SS, Khorana HG. 1990. Assembly of functional rhodopsin requires a disulfide bond between cysteine residues 110 and 187. *J. Biol. Chem.* 265:17520–24
103. Kataoka M, Kamikubo H. 2000. Structures of photointermediates and their

implications for the proton pump mechanism. *Biochim. Biophys. Acta* 1460:166–76

104. Kaushal S, Ridge KD, Khorana HG. 1994. Structure and function in rhodopsin: the role of asparagine-linked glycosylation. *Proc. Natl. Acad. Sci. USA* 91: 4024–28
105. Kelleher DJ, Johnson GL. 1988. Transducin inhibition of light-dependent rhodopsin phosphorylation: evidence for beta-gamma subunit interaction with rhodopsin. *Mol. Pharmacol.* 34:452–60
106. Kibelbek J, Mitchell DC, Beach JM, Litman BJ. 1991. Functional equivalence of metarhodopsin II and the G_t-activating form of photolyzed bovine rhodopsin. *Biochemistry* 30:6761–68
107. Kim JM, Altenbach C, Thurmond RL, Khorana HG, Hubbell WL. 1997. Structure and function in rhodopsin: Rhodopsin mutants with a neutral amino acid at E134 have a partially activated conformation in the dark state. *Proc. Natl. Acad. Sci. USA* 94:14273–78
108. Kisselev OG, Ermolaeva MV, Gautam N. 1994. A farnesylated domain in the G protein γ subunit is a specific determinant of receptor coupling. *J. Biol. Chem.* 269:21399–402
109. Kisselev O, Ermolaeva M, Gautam N. 1995. Efficient interaction with a receptor requires a specific type of prenyl group on the G protein γ subunit. *J. Biol. Chem.* 270:25356–58
110. Kisselev OG, Kao J, Ponder JW, Fann YC, Gautam N, Marshall GR. 1998. Light-activated rhodopsin induces structural binding motif in G-protein alpha subunit. *Proc. Natl. Acad. Sci. USA* 95: 4270–75
111. Kisselev OG, Meyer CK, Heck M, Ernst OP, Hofmann KP. 1999. Signal transfer from rhodopsin to the G-protein: evidence for a two-site sequential fit mechanism. *Proc. Natl. Acad. Sci. USA* 96: 4898–903
112. Kjelsberg MA, Cotecchia S, Ostrowski J, Caron MG, Lefkowitz RJ. 1992. Constitutive activation of the alpha 1β-adrenergic receptor by all amino acid substitutions at a single site. Evidence for a region which constrains receptor activation. *J. Biol. Chem.* 267:1430–33
113. Klein-Seetharaman J, Getmanova EV, Loewen MC, Reeves PJ, Khorana HG. 1999. NMR spectroscopy in studies of light-induced structural changes in mammalian rhodopsin: applicability of solution ^{19}F NMR. *Proc. Natl. Acad. Sci. USA* 96:13744–49
114. Klein-Seetharaman J, Hwa J, Cai K, Altenbach C, Hubbell WL, Khorana HG. 1999. Single-cysteine substitution mutants at amino acid positions 55–75, the sequence connecting the cytoplasmic ends of helices I and II in rhodopsin: Reactivity of the sulfhydryl groups and their derivatives identifies a tertiary structure that changes upon light-activation. *Biochemistry* 38:7938–44
115. Kliger DS, Lewis JW. 1995. Spectral and kinetic characterization of visual pigment photointermediates. *Isr. J. Chem.* 35:289–307
116. Kochendoerfer GG, Lin SW, Sakmar TP, Mathies RA. 1999. How color visual pigments are tuned. *Trends Biochem. Sci.* 24:300–5
117. Kochendoerfer GG, Verdegem PJ, van der Hoef I, Lugtenburg J, Mathies RA. 1996. Retinal analog study of the role of steric interactions in the excited state isomerization dynamics of rhodopsin. *Biochemistry* 35:16230–40
118. Kokame K, Fukada Y, Yoshizawa T, Takao T, Shimonishi Y. 1992. Lipid modification at the N terminus of photoreceptor G-protein alpha-subunit. *Nature* 359:749–52
119. Krebs A, Villa C, Edwards PC, Schertler GF. 1998. Characterization of an improved two-dimensional p22121 crystal from bovine rhodopsin. *J. Mol. Biol.* 282:991–1003
120. Lamb TD. 1996. Gain and kinetics of

activation in the G-protein cascade of phototransduction. *Proc. Natl. Acad. Sci. USA* 93:566–70
121. Lambright DG, Noel JP, Hamm HE, Sigler PB. 1994. Structural determinants for activation of the alpha-subunit of a heterotrimeric G protein. *Nature* 369: 621–28
122. Lambright DG, Sondek J, Bohm A, Skiba NP, Hamm HE, Sigler PB. 1996. The 2.0 Å crystal structure of a heterotrimeric G protein. *Nature* 379:311–19
123. Landau EM, Rosenbusch JP. 1996. Lipidic cubic phases: a novel concept for the crystallization of membrane proteins. *Proc. Natl. Acad. Sci. USA* 93:14532–35
124. Langen R, Cai K, Altenbach C, Khorana HG, Hubbell WL. 1999. Structural features of the C-terminal domain of bovine rhodopsin: a site-directed spin-labeling study. *Biochemistry* 38:7918–24
125. Le Gouill C, Parent JL, Rola-Pleszczynski M, Stankova J. 1997. Structural and functional requirements for agonist-induced internalization of the human platelet-activating factor receptor. *J. Biol. Chem.* 272:21289–95
126. Lewis JW, Kliger DS. 2000. Absorption spectroscopy in studies of visual pigments: spectral and kinetic characterization of intermediates. *Methods Enzymol.* 315:164–78
127. Lewis JW, Szundi I, Kliger DS. 2000. Structural constraints imposed by a non-native disulfide cause reversible changes in rhodopsin photointermediate kinetics. *Biochemistry* 39:7851–55
128. Lin SW, Han M, Sakmar TP. 2000. Analysis of functional microdomains of rhodopsin. *Methods Enzymol.* 315:116–30
129. Lin SW, Kochendoerfer GG, Carroll KS, Wang D, Mathies RA, Sakmar TP. 1998. Mechanisms of spectral tuning in blue cone visual pigments. Visible and Raman spectroscopy of blue-shifted rhodopsin mutants. *J. Biol. Chem.* 273:24583–91
130. Lin SW, Sakmar TP. 1996. Specific tryptophan UV-absorbance changes are probes of the transition of rhodopsin to its active state. *Biochemistry* 35:11149–59
131. Lin SW, Sakmar TP. 1999. Colour tuning mechanisms of visual pigments. *Novartis Found. Symp.* 224:124–35
132. Lin SW, Sakmar TP, Franke RR, Khorana HG, Mathies RA. 1992. Resonance Raman microprobe spectroscopy of rhodopsin mutants: effect of substitutions in the third transmembrane helix. *Biochemistry* 31:5105–11
133. Liu J, Conklin BR, Blin N, Yun J, Wess J. 1995. Identification of a receptor/G-protein contact site critical for signaling specificity and G-protein activation. *Proc. Natl. Acad. Sci. USA* 92:11642–46
134. Loew A, Ho YK, Blundell T, Bax B. 1998. Phosducin induces a structural change in transducin beta-gamma. *Structure* 6:1007–19
135. Loewen MC, Klein-Seetharaman J, Getmanova EV, Reeves PJ, Schwalbe H, Khorana HG. 2001. Solution ^{19}F nuclear Overhauser effects in structural studies of the cytoplasmic domain of mammalian rhodopsin. *Proc. Natl. Acad. Sci. USA* 98:4888–92
136. Longstaff C, Calhoon RD, Rando RR. 1986. Deprotonation of the Schiff base of rhodopsin is obligate in the activation of the G protein. *Proc. Natl. Acad. Sci. USA* 83:4209–13
137. Lou J, Tan Q, Karnaukhova E, Berova N, Nakanishi K, Crouch RK. 2000. Synthetic retinals: convenient probes of rhodopsin and visual transduction process. *Methods Enzymol.* 315:219–37
138. Luecke H. 2000. Atomic resolution structures of bacteriorhodopsin photocycle intermediates: the role of discrete water molecules in the function of this light-driven ion pump. *Biochim. Biophys. Acta* 1460:133–56
139. Luecke H, Schobert B, Richter HT, Cartailler JP, Lanyi JK. 1999. Structural changes in bacteriorhodopsin during

ion transport at 2 Å resolution. *Science* 286:255–61

140. Luecke H, Schobert B, Richter HT, Cartailler JP, Lanyi JK. 1999. Structure of bacteriorhodopsin at 1.55 Å resolution. *J. Mol. Biol.* 291:899–911
141. Marin EP, Krishna AG, Archambault V, Simuni E, Fu WY, Sakmar TP. 2001. The function of interdomain interactions in controlling nucleotide exchange rates in transducin. *J. Biol. Chem.* 276:23873–80
142. Marin EP, Krishna AG, Sakmar TP. 2001. Rapid activation of transducin by mutations distant from the nucleotide-binding site. Evidence for a mechanistic model of receptor-catalyzed nucleotide exchange by G proteins. *J. Biol. Chem.* 276:27400–5
143. Marin EP, Krishna AG, Zvyaga TA, Isele J, Siebert F, Sakmar TP. 2000. The amino terminus of the fourth cytoplasmic loop of rhodopsin modulates rhodopsin-transducin interaction. *J. Biol. Chem.* 275:1930–36
144. Marin EP, Neubig RR. 1995. Lack of association of G-protein beta 2- and gamma 2-subunit N-terminal fragments provides evidence against the coiled-coil model of subunit-beta gamma assembly. *Biochem. J.* 309:377–80
145. Matsuda T, Hashimoto Y, Ueda H, Asano T, Matsuura Y, et al. 1998. Specific isoprenyl group linked to transducin gamma-subunit is a determinant of its unique signaling properties among G-proteins. *Biochemistry* 37:9843–50
146. Matsumura H, Shiba T, Inoue T, Harada S, Kai Y. 1998. A novel mode of target recognition suggested by the 2.0 Å structure of holo S100B from bovine brain. *Structure* 6:233–41
147. McDowell JH, Nawrocki JP, Hargrave PA. 1993. Phosphorylation sites in bovine rhodopsin. *Biochemistry* 32:4968–74
148. Meng EC, Bourne HR. 2001. Receptor activation: What does the rhodopsin structure tell us? *Trends Pharmacol. Sci.* 22:587–93
149. Menon ST, Han M, Sakmar TP. 2001. Rhodopsin: structural basis of molecular physiology. *Physiol. Rev.* 81:1659–88
150. Milburn MV, Prive GG, Milligan DL, Scott WG, Yeh J, et al. 1991. Three-dimensional structures of the ligand-binding domain of the bacterial aspartate receptor with and without a ligand. *Science* 254:1342–47
151. Min KC, Gravina SA, Sakmar TP. 2000. Reconstitution of the vertebrate visual cascade using recombinant heterotrimeric transducin purified from Sf9 cells *Protein Exp. Purif.* 20:514–26

151a. Moore WJ. 1972. *Physical Chemistry*. Englewood Cliffs, NJ: Prentice Hall. 977 pp.

152. Murata K, Fujii Y, Enomoto N, Hata M, Hoshino T, Tsuda M. 2000. A study on the mechanism of the proton transport in bacteriorhodopsin: the importance of the water molecule. *Biophys. J.* 79:982–91
153. Nagata T, Terakita A, Kandori H, Kojima D, Shichida Y, Maeda A. 1997. Water and peptide backbone structure in the active center of bovine rhodopsin. *Biochemistry* 36:6164–70
154. Nakayama TA, Khorana HG. 1990. Orientation of retinal in bovine rhodopsin determined by cross-linking using a photoactivatable analog of 11-*cis*-retinal. *J. Biol. Chem.* 265:15762–69
155. Nakayama TA, Khorana HG. 1991. Mapping of the amino acids in membrane-embedded helices that interact with the retinal chromophore in bovine rhodopsin. *J. Biol. Chem.* 266:4269–75
156. Nathans J. 1990. Determinants of visual pigment absorbance: role of charged amino acids in the putative transmembrane segments. *Biochemistry* 29:937–42
157. Nathans J, Hogness DS. 1983. Isolation, sequence analysis, and intron-exon arrangement of the gene encoding bovine rhodopsin. *Cell* 34:807–14

158. Nathans J, Hogness DS. 1984. Isolation and nucleotide sequence of the gene encoding human rhodopsin. *Proc. Natl. Acad. Sci. USA* 81:4851–55
159. Natochin M, Granovsky AE, Muradov KG, Artemyev NO. 1999. Roles of the transducin alpha-subunit alpha4-helix/alpha4-beta6 loop in the receptor and effector interactions. *J. Biol. Chem.* 274: 7865–69
160. Neer EJ, Schmidt CJ, Nambudripad R, Smith TF. 1994. The ancient regulatory-protein family of WD-repeat proteins. *Nature* 371:297–300
161. Neitz M, Neitz J, Jacobs GH. 1991. Spectral tuning of pigments underlying red-green color vision. *Science* 252:971–74
162. Neutze R, Hajdu J. 1997. Femtosecond time resolution in X-ray diffraction experiments. *Proc. Natl. Acad. Sci. USA* 94:5651–55
163. Nishimura S, Kandori H, Maeda A. 1998. Interaction between photoactivated rhodopsin and the C-terminal peptide of transducin alpha-subunit studied by FTIR spectroscopy. *Biochemistry* 37:15816–24
164. Noel JP, Hamm HE, Sigler PB. 1993. The 2.2 Å crystal structure of transducin-alpha complexed with GTPγS. *Nature* 366:654–63
165. Ohguro H, Palczewski K, Ericsson LH, Walsh KA, Johnson RS. 1993. Sequential phosphorylation of rhodopsin at multiple sites. *Biochemistry* 32:5718–24
166. Ohguro H, Rudnicka-Nawrot M, Buczylko J, Zhao X, Taylor JA, et al. 1996. Structural and enzymatic aspects of rhodopsin phosphorylation. *J. Biol. Chem.* 271:5215–24
167. Okada T, Le Trong I, Fox BA, Behnke CA, Stenkamp RE, Palczewski K. 2000. X-ray diffraction analysis of three-dimensional crystals of bovine rhodopsin obtained from mixed micelles. *J. Struct. Biol.* 130:73–80
168. Okada T, Takeda K, Kouyama T. 1998. Highly selective separation of rhodopsin from bovine rod outer segment membranes using combination of divalent cation and alkyl(thio)glucoside. *Photochem. Photobiol.* 67:495–99
169. Oprian DD. 1992. The ligand-binding domain of rhodopsin and other G protein-linked receptors. *J. Bioenerg. Biomembr.* 24:211–17
170. Osawa S, Weiss ER. 1995. The effect of carboxyl-terminal mutagenesis of G_t alpha on rhodopsin and guanine nucleotide binding. *J. Biol. Chem.* 270:31052–58
171. Ovchinnikov YUA. 1982. Rhodopsin and bacteriorhodopsin: structure-function relationships. *FEBS Lett.* 148:179–91
172. Palczewski K, Kumasaka T, Hori T, Behnke CA, Motoshima H, et al. 2000. Crystal structure of rhodopsin: a G protein-coupled receptor. *Science* 289: 739–45
173. Palings I, Pardoen JA, van den Berg E, Winkel C, Lugtenburg J, Mathies RA. 1987. Assignment of fingerprint vibrations in the resonance Raman spectra of rhodopsin, isorhodopsin, and bathorhodopsin: implications for chromophore structure and environment. *Biochemistry* 26:2544–56
174. Papac DI, Oatis JE Jr, Crouch RK, Knapp DR. 1993. Mass spectrometric identification of phosphorylation sites in bleached bovine rhodopsin. *Biochemistry* 32:5930–34
175. Papermaster DS. 1982. Preparation of retinal rod outer segments. *Methods Enzymol.* 81:48–52
176. Pappa H, Murray-Rust J, Dekker LV, Parker PJ, McDonald NQ. 1998. Crystal structure of the C2 domain from protein kinase C-delta. *Structure* 6:885–94
177. Pebay-Peyroula E, Neutze R, Landau EM. 2000. Lipidic cubic phase crystallization of bacteriorhodopsin and cryotrapping of intermediates: towards resolving a revolving photocycle. *Biochim. Biophys. Acta* 1460:119–32

178. Phillips WJ, Cerione RA. 1992. Rhodopsin-transducin interaction. I. Characterization of the binding of the transducin-beta gamma subunit complex to rhodopsin using fluorescence spectroscopy. *J. Biol. Chem.* 267:17032–39
179. Phillips WJ, Wong SC, Cerione RA. 1992. Rhodopsin-transducin interactions. II. Influence of the transducin-beta gamma subunit complex on the coupling of the transducin-alpha subunit to rhodopsin. *J. Biol. Chem.* 267:17040–46
180. Popp A, Ujj L, Atkinson GH. 1996. Bathorhodopsin structure in the room-temperature rhodopsin photosequence: picosecond time-resolved coherent anti-Stokes Raman scattering. *Proc. Natl. Acad. Sci. USA* 93:372–76
181. Probst WC, Snyder LA, Schuster DI, Brosius J, Sealfon SC. 1992. Sequence alignment of the G-protein coupled receptor superfamily. *DNA Cell. Biol.* 11: 1–20
182. Rafferty CN, Muellenberg CG, Shichi H. 1980. Tryptophan in bovine rhodopsin: its content, spectral properties and environment. *Biochemistry* 19:2145–51
183. Rando RR. 1996. Polyenes and vision. *Chem. Biol.* 3:255–62
184. Rao VR, Cohen GB, Oprian DD. 1994. Rhodopsin mutation G90D and a molecular mechanism for congenital night blindness. *Nature* 367:639–42
185. Rao VR, Oprian DD. 1996. Activating mutations of rhodopsin and other G protein-coupled receptors. *Annu. Rev. Biophys. Biomol. Struct.* 25:287–314
186. Rath P, DeCaluwe LL, Bovee-Geurts PH, DeGrip WJ, Rothschild KJ. 1993. Fourier transform infrared difference spectroscopy of rhodopsin mutants: Light activation of rhodopsin causes hydrogen-bonding change in residue aspartic acid-83 during meta II formation. *Biochemistry* 32:10277–82
187. Resek JF, Farahbakhsh ZT, Hubbell WL, Khorana HG. 1993. Formation of the meta II photointermediate is accompanied by conformational changes in the cytoplasmic surface of rhodopsin. *Biochemistry* 32:12025–32
188. Ridge KD, Bhattacharya S, Nakayama TA, Khorana HG. 1992. Light-stable rhodopsin. II. An opsin mutant (TRP-265 → Phe) and a retinal analog with a nonisomerizable 11-*cis* configuration form a photostable chromophore. *J. Biol. Chem.* 267:6770–75
189. Robinson PR, Cohen GB, Zhukovsky EA, Oprian DD. 1992. Constitutively active mutants of rhodopsin. *Neuron* 9: 719–25
190. Rothschild KJ. 1992. FTIR difference spectroscopy of bacteriorhodopsin: toward a molecular model. *J. Bioenerg. Biomembr.* 24:147–67
191. Saito H, Tuzi S, Yamaguchi S, Tanio M, Naito A. 2000. Conformation and backbone dynamics of bacteriorhodopsin revealed by ^{13}C-NMR. *Biochim. Biophys. Acta* 1460:39–48
192. Sakmar TP. 1994. Opsins. In *Handbook of Receptors and Channels: G Protein Coupled Receptors*, ed. SJ Peroutka, pp. 257. Boca Raton, FL: CRC
193. Sakmar TP. 1998. Rhodopsin: a prototypical G protein-coupled receptor. *Prog. Nucleic Acid Res. Mol. Biol.* 59:1–34
194. Sakmar TP. 2002. The structure of rhodopsin and the superfamily of seven-helical receptors: the same and not the same. *Curr. Opin. Cell Biol.* 14:189–95
195. Sakmar TP, Fahmy K. 1995. Properties and photoactivity of rhodopsin mutants. *Isr. J. Chem.* 35:325–37
196. Sakmar TP, Franke RR, Khorana HG. 1989. Glutamic acid-113 serves as the retinylidene Schiff base counterion in bovine rhodopsin. *Proc. Natl. Acad. Sci. USA* 86:8309–13
197. Sass HJ, Büldt G, Gessenich R, Hehn D, Neff D, et al. 2000. Structural alterations for proton translocation in the M state of wild-type bacteriorhodopsin. *Nature* 406:649–53

198. Scheer A, Gierschik P. 1995. S-prenylated cysteine analogues inhibit receptor-mediated G protein activation in native human granulocyte and reconstituted bovine retinal rod outer segment membranes. *Biochemistry* 34:4952–61
199. Schertler GF, Villa C, Henderson R. 1993. Projection structure of rhodopsin. *Nature* 362:770–72
200. Sheikh SP, Zvyaga TA, Lichtarge O, Sakmar TP, Bourne HR. 1996. Rhodopsin activation blocked by metal-ion-binding sites linking transmembrane helices C and F. *Nature* 383:347–50
201. Siebert F. 1995. Applications of FTIR spectroscopy to the investigation of dark structures and photoreactions of visual pigments. *Isr. J. Chem.* 35:309–23
202. Singh D, Hudson BS, Middleton C, Birge RR. 2001. Conformation and orientation of the retinyl chromophore in rhodopsin: A critical evaluation of recent NMR data on the basis of theoretical calculations results in a minimum energy structure consistent with all experimental data. *Biochemistry* 40:4201–4
203. Slep KC, Kercher MA, He W, Cowan CW, Wensel TG, Sigler PB. 2001. Structural determinants for regulation of phosphodiesterase by a G protein at 2.0 Å. *Nature* 409:1071–77
204. Sondek J, Bohm A, Lambright DG, Hamm HE, Sigler PB. 1996. Crystal structure of a G-protein beta gamma dimer at 2.1 Å resolution. *Nature* 379: 369–74
205. Sondek J, Lambright DG, Noel JP, Hamm, HE, Sigler PB. 1994. GTPase mechanism of G proteins from the 1.7 Å crystal structure of transducin alpha-GDP-AIF4. *Nature* 372:276–79
206. Sprang SR. 1997. G protein mechanisms: insights from structural analysis. *Annu. Rev. Biochem.* 66:639–78
207. Strader CD, Fong TM, Tota MR, Underwood D, Dixon RA. 1994. Structure and function of G protein-coupled receptors. *Annu. Rev. Biochem.* 63:101–32
208. Struthers M, Yu H, Kono M, Oprian DD. 1999. Tertiary interactions between the fifth and sixth transmembrane segments of rhodopsin. *Biochemistry* 38:6597–603
209. Struthers M, Yu H, Oprian DD. 2000. G protein-coupled receptor activation: analysis of a highly constrained "strait-jacketed" rhodopsin. *Biochemistry* 39: 7938–42
210. Stryer L. 1988. Molecular basis of visual excitation. *Cold Spring Harb. Symp. Quant. Biol.* 53:283–94
211. Stryer L. 1991. Visual excitation and recovery. *J. Biol. Chem.* 266:10711–14
212. Subramaniam S, Gerstein M, Oesterhelt D, Henderson R. 1993. Electron diffraction analysis of structural changes in the photocycle of bacteriorhodopsin. *EMBO J.* 12:1–8
213. Subramaniam S, Henderson R. 2000. Molecular mechanism of vectorial proton translocation by bacteriorhodopsin. *Nature* 406:653–57
214. Subramaniam S, Lindahl M, Bullough P, Faruqi AR, Tittor J, et al. 1999. Protein conformational changes in the bacteriorhodopsin photocycle. *J. Mol. Biol.* 287:145–61
215. Surya A, Foster KW, Knox BE. 1995. Transducin activation by the bovine opsin apoprotein. *J. Biol. Chem.* 270: 5024–31
216. Sutton RB, Sprang SR. 1998. Structure of the protein kinase C beta phospholipid-binding C2 domain complexed with Ca^{2+}. *Structure* 6:1395–405
217. Taylor JM, Jacob-Mosier GG, Lawton RG, VanDort M, Neubig RR. 1996. Receptor and membrane interaction sites on G beta. A receptor-derived peptide binds to the carboxyl terminus. *J. Biol. Chem.* 271:3336–39
218. Teller DC, Okada T, Behnke CA, Palczewski K, Stenkamp RE. 2001. Advances in determination of a high-resolution three-dimensional structure of

rhodopsin, a model of G-protein-coupled receptors (GPCRs). *Biochemistry* 40: 7761–72
219. Unger VM, Hargrave PA, Baldwin JM, Schertler GF. 1997. Arrangement of rhodopsin transmembrane alpha-helices. *Nature* 389:203–6
220. Verdaguer N, Corbalan-Garcia S, Ochoa WF, Fita I, Gomez-Fernandez JC. 1999. Ca^{2+} bridges the C2 membrane-binding domain of protein kinase C alpha directly to phosphatidylserine. *EMBO J.* 18:6329–38
221. Verdegem PJ, Bovee-Geurts PH, de Grip WJ, Lugtenburg J, de Groot HJ. 1999. Retinylidene ligand structure in bovine rhodopsin, metarhodopsin-I, and 10-methylrhodopsin from internuclear distance measurements using ^{13}C-labeling and 1-D rotational resonance MAS-NMR. *Biochemistry* 38:11316–24
222. Verhoeven MA, Creemers AF, Bovee-Geurts PH, De Grip WJ, Lugtenburg J, de Groot HJ. 2001. Ultra-high-field MAS NMR assay of a multispin labeled ligand bound to its G-protein receptor target in the natural membrane environment: electronic structure of the retinylidene chromophore in rhodopsin. *Biochemistry* 40:3282–88
223. Wald G. 1968. Molecular basis of visual excitation. *Science* 162:230–39
224. Wang Q, Schoenlein WR, Peteanu LA, Mathies RA, Shank CV. 1994. Vibrationally coherent photochemistry in the femtosecond primary event of vision. *Science* 266:422–24
225. Wang Z, Asenjo AB, Oprian DD. 1993. Identification of the Cl^--binding site in the human red and green color vision pigments. *Biochemistry* 32:2125–30
226. Wedegaertner PB, Wilson PT, Bourne HR. 1995. Lipid modifications of trimeric G proteins. *J. Biol. Chem.* 270: 503–6
227. Wilson MA, Brunger AT. 2000. The 1.0 Å crystal structure of Ca^{2+}-bound calmodulin: an analysis of disorder and implications for functionally relevant plasticity. *J. Mol. Biol.* 301:1237–56
228. Yamashita T, Terakita A, Shichida Y. 2000. Distinct roles of the second and the third cytoplasmic loops of bovine rhodopsin in G protein activation. *J. Biol. Chem.* 275:34272–79
229. Yau KW, Matthews G, Baylor DA. 1979. Thermal activation of the visual transduction mechanism in retinal rods. *Nature* 279:806–7
230. Yu H, Kono M, Oprian DD. 1999. State-dependent disulfide cross-linking in rhodopsin. *Biochemistry* 38:12028–32
231. Yu H, Oprian DD. 1999. Tertiary interactions between transmembrane segments 3 and 5 near the cytoplasmic side of rhodopsin. *Biochemistry* 38:12033–40
232. Zhang H, Lerro KA, Yamamoto T, Lien TH, Sastry L, et al. 1994. The location of the chromophore in rhodopsin—a photoaffinity study. *J. Am. Chem. Soc.* 116:10165–73
233. Zhukovsky EA, Oprian DD. 1989. Effect of carboxylic acid side chains on the absorption maximum of visual pigments. *Science* 246:928–30
234. Zhukovsky EA, Robinson PR, Oprian DD. 1991. Transducin activation by rhodopsin without a covalent bond to the 11-*cis*-retinal chromophore. *Science* 251:558–60
235. Zvyaga TA, Fahmy K, Siebert F, Sakmar TP. 1996. Characterization of the mutant visual pigment responsible for congenital night blindness: a biochemical and Fourier-transform infrared spectroscopy study. *Biochemistry* 35:7536–45